Electronic Supplementary Material (ESI) for ChemComm.

Supporting Information

Robust supramolecular nanocylinders of naphthalene-diimide in water

*Thomas Choisnet, David Canevet, Marc Sallé, Erwan Nicol, Frédérick Niepceron, Jacques Jestin, and Olivier Colombani**

1 Synthesis

1.1 Materials.

Analytical grade solvents were purchased from Aldrich and dried whenever necessary according to standard procedures (sodium/benzophenone or CaH_2 for tetrahydrofuran (THF), CaH_2 for dichloromethane and methanol). 1,4,5,8-Naphthalenetetracarboxylic dianhydride (Aldrich), ethylamine (Aldrich, 66-72% in H_2O) , N-Boc-ethylenediamine (Aldrich, 98%), N,N-diisopropylethylamine (Aldrich, 99%), trifluoroacetic acid (Alfa Aesar, 99%), 2,4-dimethyl-5-nitroaniline (Combi-Blocks, 98%), 4-butylphenyle isocyanate (Aldrich, 97%), 10% Pd on carbon (Aldrich, 97%), triphosgene (Acros Organics, 99%), triethylamine (Aldrich, 99%), butan-1-amine (Aldrich, 99.5%) were used as received. POE-NH_2 was synthesized from a commercial methoxypolyethylene glycol 2000 (Aldrich) according to Mongondry *et al.*[1]

Thin-Layer Chromatography (TLC) was performed on aluminium plates coated with Merck Silica gel 60 F254. Developed plates were air-dried and scrutinized under a UV lamp. Silica gel (Sigma Aldrich, SiO_2, pore size 60 Å, 40-63 μm technical grades) was used for preparative silica gel chromatography. Bio-Beads S-X3 support (BIO-RAD, porous styrene divinylbenzene 40–80 μm bead size, ≤2000 g/mol M_W limit) was used for preparative size exclusion chromatography.

1.2 Characterization.

Nuclear Magnetic Resonance (NMR) spectra were recorded using deuterated chloroform ($CDCl_3$) or dimethyl sulfoxide (DMSO-D_6) as solvents either on a BRUKER advance DPX 200 operating at 200 MHz for ^1H, a BRUKER advance DRX 300 operating at 300 MHz for ^1H NMR and 75 MHz for ^{13}C NMR or on a BRUKER AC-400 spectrometer operating at 400 MHz for ^1H NMR and 100 MHz for ^{13}C NMR. Coupling constants (J) are denoted in Hz and chemical shifts (δ) in parts per million (ppm) relative to TMS. Multiplicities are denoted as follows: s = singlet, d = doublet, t = triplet, q = quartet, qt = quintuplet, hx = hexuplet, m = multiplet.

Size Exclusion Chromatography (SEC). Polymers were characterized on a SEC system operating in *N,N*-dimethylformamide (DMF) 99+% extra pure eluent containing LiBr (1 g/L) at 60 °C. The apparatus consisted of a guard column (PL gel 5μm) and two Polymer Laboratories PL mixed-d columns, a Waters 410 differential refractometer (DRI) and a Waters 996 UV-Visible photodiode array detector. The instrument operated at a flow rate of 1.0 $mL.min^{-1}$ and was calibrated with narrow linear poly(methyl methacrylate) (PMMA) standards ranging in molar mass from 904 $g.mol^{-1}$ to 304 000 $g.mol^{-1}$. The PMMA-equivalent average molar masses (number-average molar mass M_n, weight-average molar mass M_w) and dispersity ($Đ = M_w/M_n$) values were calculated using Waters EMPOWER software based on the DRI signal.

Matrix-Assisted Laser Desorption and Ionization-Time Of Flight (MALDI-TOF) mass spectrometry analysis was performed either on a Bruker Reflex III spectrometer operating in linear mode or on a Bruker UltraFlex II instrument equipped with a nitrogen laser operating at 337 nm, pulsed ion extraction source and reflectron. Spectra were recorded for both devices in the linear or reflectron mode with an acceleration voltage of 19 kV and a delay of 200 ns. 500 single shot acquisitions were summed to give the spectra, which were analyzed using the FlexAnalysis software. Different matrices were used as detailed in the characterization part. Samples were prepared by mixing the polymer, the matrix and the solvent, and evaporating a few drops of the solution on the analysis grid.

Dual Stage Quadrupole GC/MS (DSQ) analysis was performed on a Thermo Scientific DSQ™ II Series Single Quadrupole GC/MS Mass Spectrometer with direct introduction.

Elemental analysis (EA) was performed on a Thermo Scientific flash 2000 elemental analyzer.

1.3 Experimental details.

1.3.1 PEO-NDI.

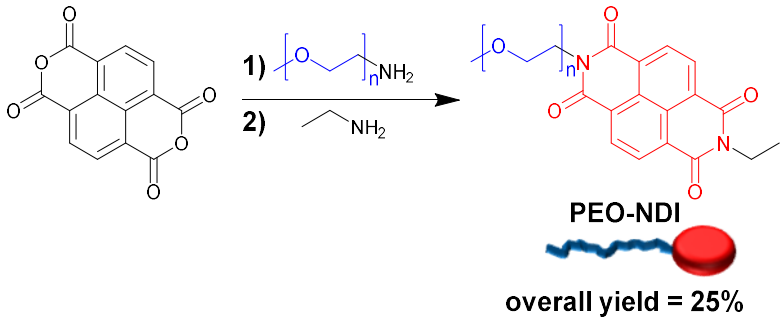

Scheme S1. Synthetic scheme of **PEO-NDI**

In a 100 mL double-necked round bottom flask, 1,4,5,8-naphthalenetetracarboxylic dianhydride (NDA) (1.342 g, 5 mmol, 19.1 eq.) was dissolved in DMF (10 mL) and heated to reflux. A PEO-NH_2 solution (0.524 g, 0.262 mmol, 1 eq.) in DMF (10 mL) was added dropwise and the mixture was further heated to reflux overnight. The black reaction mixture was then cooled to room temperature, concentrated under vacuum, dispersed in hot chloroform and then filtered through celite on a sintered glass funnel to remove the major part of excess NDA. The solvent was evaporated *in vacuo*. Ethylamine (2.2 mL, 26.1 mmol, 104 eq.), trimethylamine (3.3 mL, 24.4 mmol, 98 eq.) and DMF (20 mL) were added and the mixture was heated to reflux overnight.

Attempts to remove impurities (unreacted NDA or PEO-NDA monoadduct as well as excess reagents) by dissolving the crude polymer in toluene and then washing it with water, filtering it or precipitating it in diethyl ether/pentane (50/50 v/v) were unsuccessful. The crude product was finally purified by size exclusion chromatography (Bio-Beads, M_w<2000 g/mol) with chloroform stabilized with ethanol as eluent, followed by two precipitations in a cold 1/1 mixture of pentane/diethyl ether. This procedure yielded **PEO-NDI** as a dark brown solid (0.14 g, 0.066 mmol, **25%**). However, the ^{1}H NMR spectrum (see **Figure S1**) shows an integral value for the PEO main-chain protons higher than expected suggesting that ~ 50 wt% of non-functional PEO is still present in the final compound. This amount of non-functional PEO was taken into account for the light scattering experiments.

^{1}H NMR (400 MHz, $CDCl_3$), **Figure S1**, δ (ppm) = 8.75 (s, $4H_f$), 4.45 (t, J = 5.8 Hz, $2H_e$), 4.27 (q, J = 7 Hz, $2H_g$), 3.90-3.05 (m, $2H_d + 2H_b \times DP_n + 2H_c \times DP_n + 3H_a$ + non functional PEO), 1.35 (t, J = 7 Hz, $3H_e$).

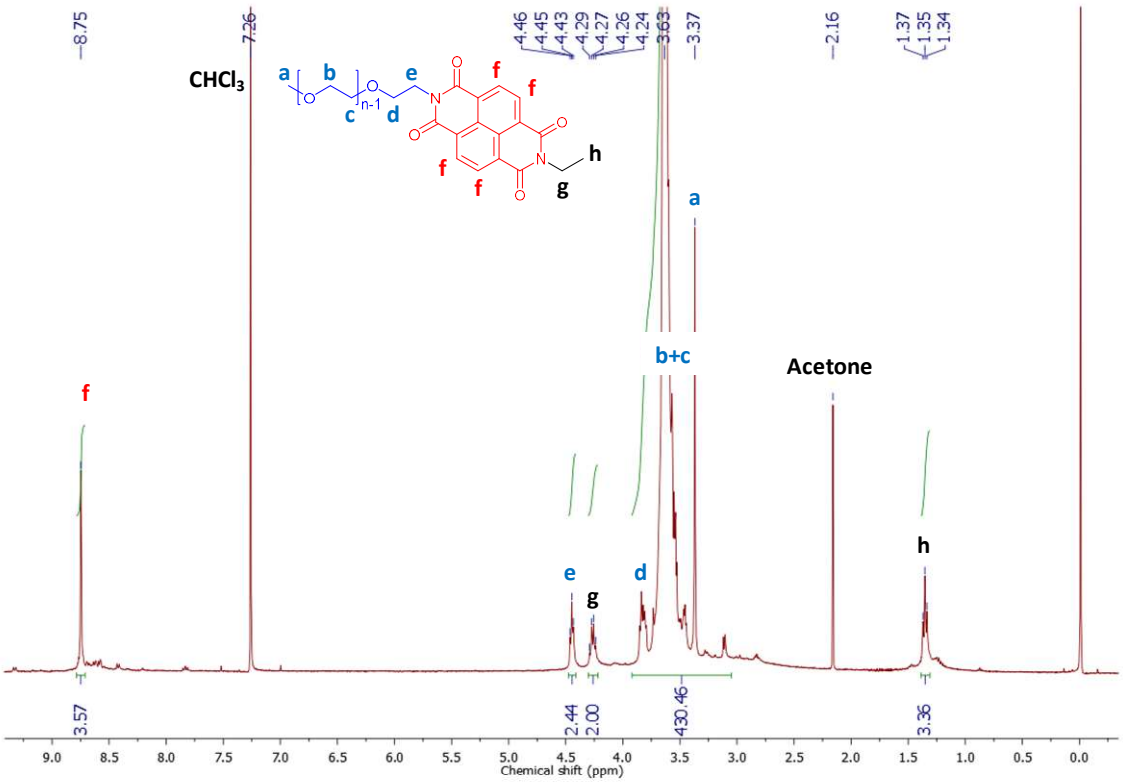

Figure S1. ^{1}H NMR spectrum of **PEO-NDI** in $CDCl_3$

MALDI-TOF MS (Dithranol (DIT), Na^+), **Figure S2**: M_{exp} (for n = 42) = 2180.23 g/mol, M_{th} (for n = 42) =2180.16 g/mol.

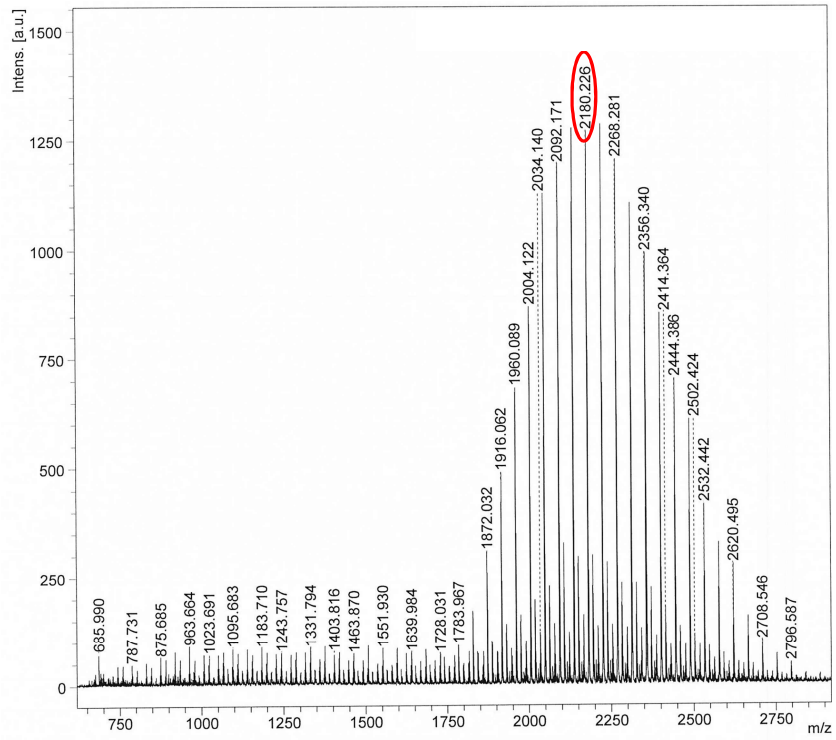

Figure S2. MALDI-TOF of **PEO-NDI** with dithranol used as matrix and NaTFA used as salt.

1.3.2 PEO-NDI-U_2.

The architecture of **PEO-NDI-U_2** was designed to induce self-assembly as mentioned in the manuscript. One of the challenges was the selective functionalization of both sides of the naphthalene dianhydride (NDA), respectively with a PEO arm and a bis(urea) moiety. This was done using a convergent synthesis route depicted in **Scheme S2**.

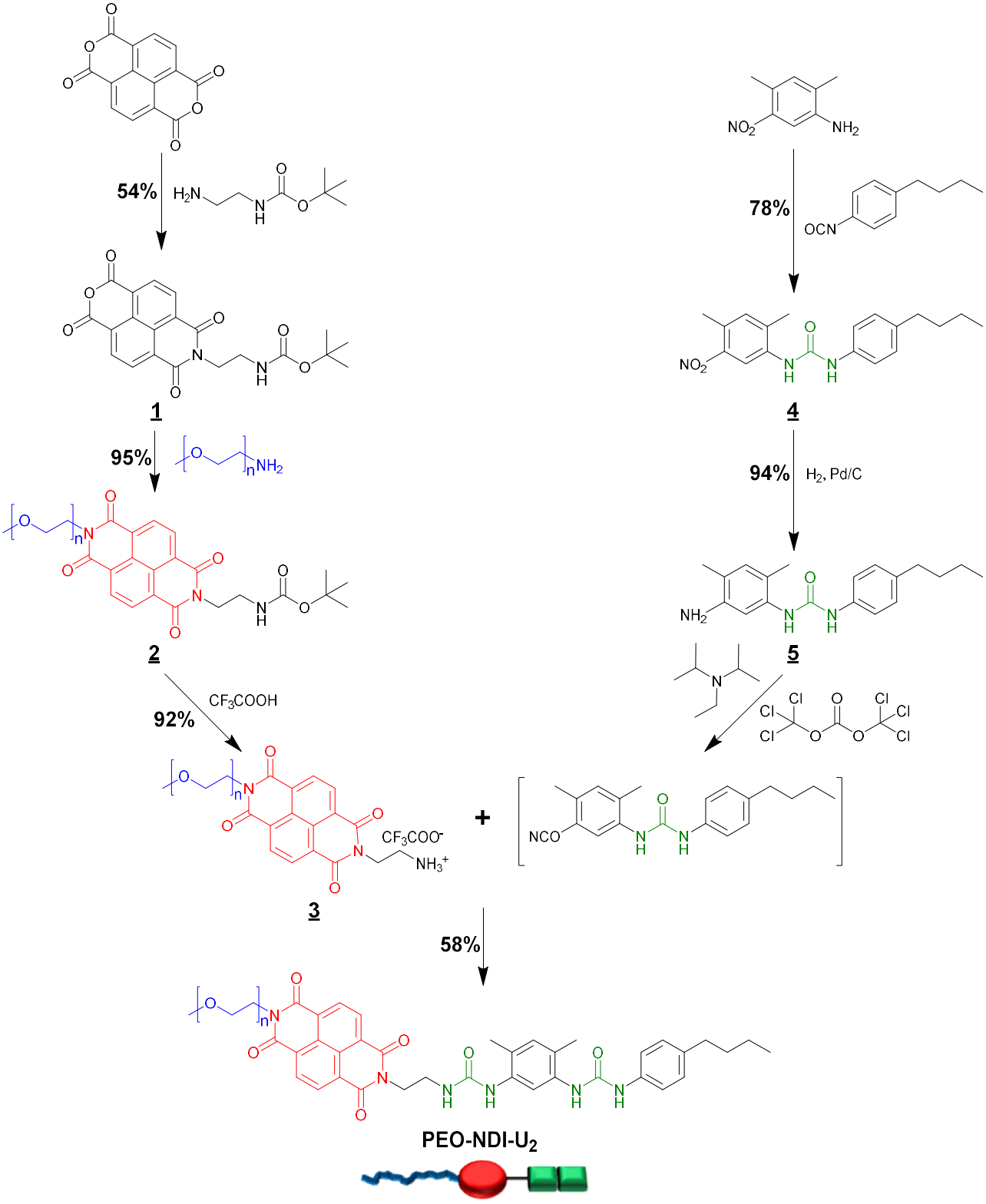

Scheme S2. Synthesis of **PEO-NDI-U_2**

Synthesis of 1:

Naphthalene dianhydride was first reacted with Boc-protected ethylene diamine in the presence of diisopropylethylamine to form the monoimide intermediate **1** following a procedure described by Iverson et *al*.[2]

In a round bottom flask, 1,4,5,8-naphthalenetetracarboxylic dianhydride (1.291 g, 4.81 mmol, 1.09 eq.), was suspended in DMF (25 mL) and *N*-Boc-ethylenediamine (0.7 mL, 4.4 mmol, 1 eq.) in THF (2 mL) was added. The reaction mixture was sonicated for 5 min and then heated under microwave irradiation in the open reaction vessel fitted with a reflux condenser at 75 °C (200 W) for 5 min and then 140 °C (250 W) for 15 min. The red cloudy reaction mixture was cooled to room temperature and the solvent was removed under vacuum. The crude product was then dissolved in chloroform, filtered and purified on a recycling preparative HPLC with $CHCl_3$ (stabilized with ethanol) to yield a yellow solid (0.97 g, 2.4 mmol, **54%**).

^{1}H NMR (300 MHz, DMSO-D_6), **Figure S3**, δ (ppm) = 8.70 (m, $4H_e$), 6.94 (t, J = 6 Hz, H_b), 4.16 (t, J = 5.5 Hz, $2H_d$), 3.30 (m, $2H_c$), 1.23 (s, $9H_a$).

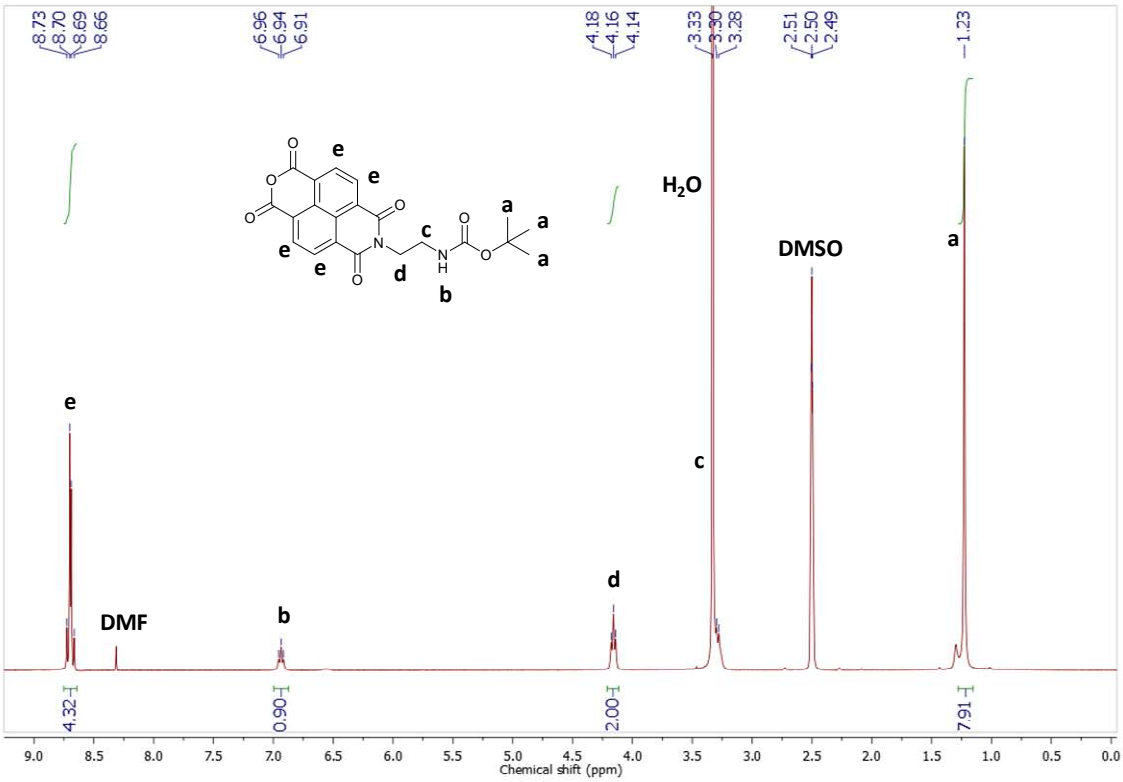

Figure S3. ^{1}H NMR spectrum of **1** in DMSO-D_6

^{13}C NMR (100 MHz, DMSO-D_6), **Figure S4**, δ (ppm) = 162.5, 159.7, 155.8, 131.8, 130.2, 128.4, 127.3, 126.2, 123.6, 77.5, 40.4, 37.6, 28.1.

The ^{13}C NMR was measured several months after the synthesis of **1**. We speculate that the small peaks at 168.5, 163.0, 129.8, 79.2 and 30.7 ppm result from partial hydrolysis of the anhydride function of **1**.

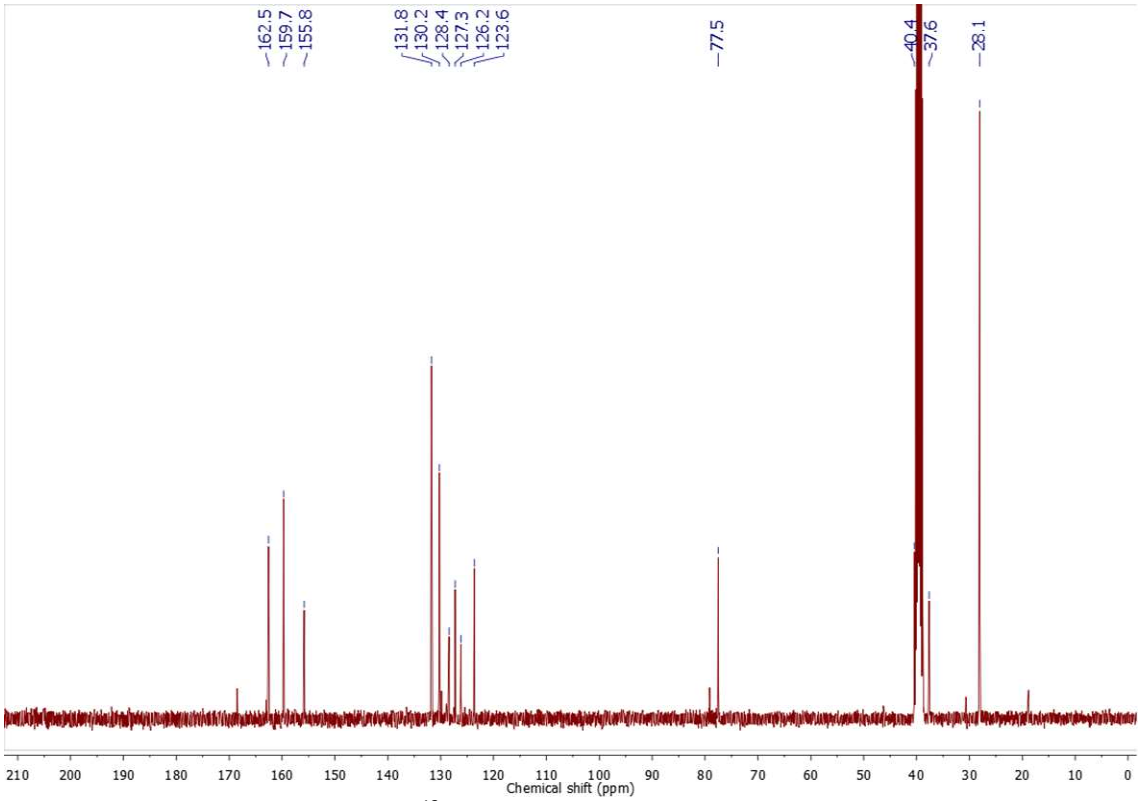

Figure S4. ^{13}C NMR spectrum of **1** in DMSO-D_6

MALDI-TOF MS (*trans*-2-[3-(4-*tert*-Butylphenyl)-2-methyl-2-propenylidene] malononitrile (DCTB), -H): M_{exp} = 409.30 g/mol, M_{th} = 409.10 g/mol.

EA: theoretical % (C = 61.5, H = 4.4, N = 6.8), experimental % (C = 59.6, H = 4.2, N = 6.4).

Synthesis of 2:

In a 250 mL round bottom flask, **1** (0.949 g, 2.3 mmol, 1 eq.), PEO-NH_2 (4.263 g, 2.1 mmol, 0.92 eq.), and diisopropylethylamine (DIEA) (0.4 mL, 2.30 mmol, 0.99 eq.) were dissolved in dry DMF (100 mL). The reaction mixture was heated at 90 °C during two days. After evaporation of the solvent, the residue was dissolved in a small amount of chloroform and precipitated in a 1/1 mixture of ice-cold pentane/diethyl ether. After filtration and drying under vacuum, a brown powder was obtained (4.897 g, 2.2 mmol, **95%**).

^{1}H NMR (400 MHz, $CDCl_3$), **Figure S5**, δ (ppm) = 8.78-8.72 (m, $4H_f$), 4.87 (t, H_i), 4.44 (t, J = 5.9 Hz, $2H_e$), 4.37 (t, J = 5.7 Hz, $2H_g$), 3.90-3.20 (m, 240H ~ $2H_b \times DP_n + 2H_c \times DP_n + 2H_d + 2H_h$), 3.36 (s, $3H_a$), 1.22 (s, $9H_j$).

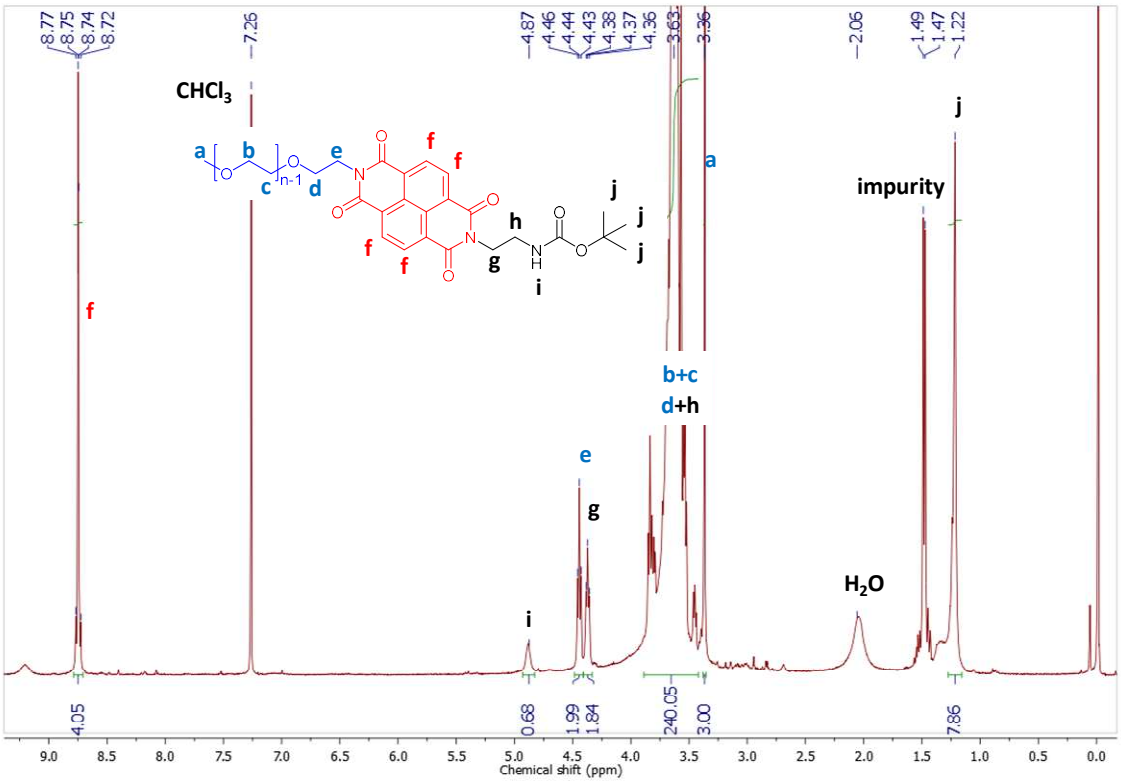

Figure S5. ^{1}H NMR spectrum of **2** in $CDCl_3$

MALDI-TOF MS (Dithranol (DIT), Na^+), **Figure S6**: M_{exp} (for n = 41) = 2251.26 g/mol, M_{th} (for n = 41) = 2251.17 g/mol.

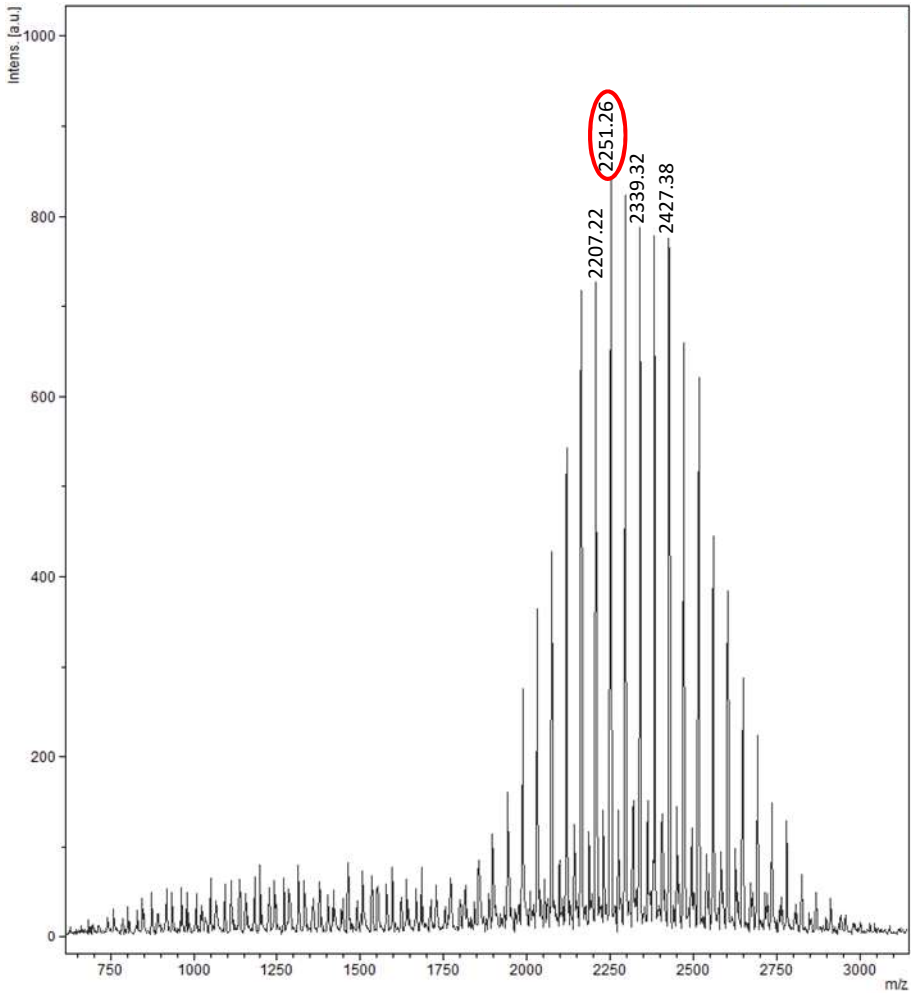

Figure S6. MALDI-TOF of **2** with dithranol used as matrix without salt addition

Synthesis of 3:

The protective Boc function of **2** was then removed by reaction with a large excess of trifluoroacetic acid in dichloromethane (60:1) according to a procedure derived from Bezençon *et al.*[3] leading to **3**.

In a round bottom flask, **2** (4.286 g, 1.85 mmol,1 eq.) was dissolved in dichloromethane before the addition of trifluoroacetic acid (TFA) (8.5 mL, 110 mmol, 60 eq.). The reaction mixture was stirred for 24 h at room temperature, then concentrated under reduced pressure and precipitated in a 1/1 mixture of pentane and diethyl ether. The resulting product was collected by filtration and dried *in vacuo* (3.98 g, 1.8 mmol, **92%**) as a brown powder.

^{1}H NMR (400 MHz, $CDCl_3$), **Figure S7**, δ (ppm) = 8.80-8.68 (m, $4H_f$), 7.80 (s, $3H_i$), 4.55-4.41 (m, $2H_g$ + $2H_e$), 3.95-3.30 (m, 165H ~ $2H_b \times DP_n + 2H_c \times DP_n + 2H_d + 2H_h$), 3.37 (s, $3H_a$).

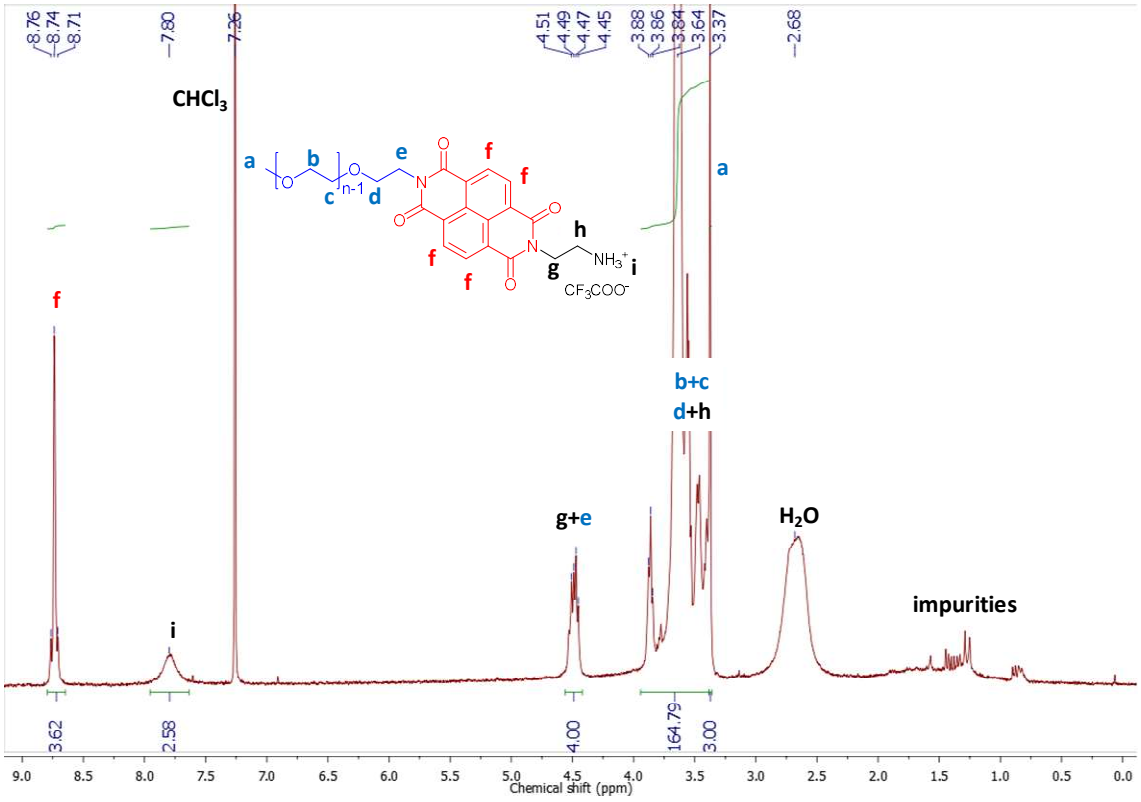

Figure S7. ^{1}H NMR spectrum of **3** in $CDCl_3$

MALDI-TOF MS (2-(4-Hydroxyphenylazo)benzoic acid (HABA), Na^+), **Figure S8**:
M_{exp} (for n = 42) = 2195.00 g/mol, M_{th} (for n = 42) = 2195.17 g/mol for **3** terminated by a NH_2 function rather than a NH_3^+, CF_3COO^- and associated with a Na^+ counter-ion.

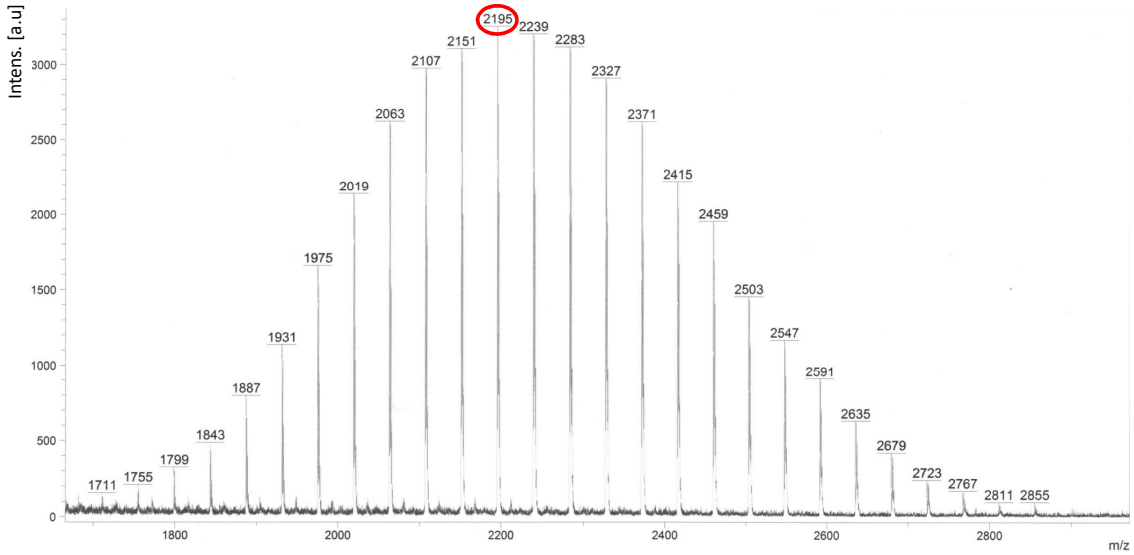

Figure S8. MALDI-TOF of **3** with 2-(4-Hydroxyphenylazo)benzoic acid used as matrix without salt addition

Synthesis of 1-(4-butylphenyl)-3-(2,4-dimethyl-5-nitrophenyl)urea (4):

In a schlenk flask, 2,4-dimethyl-5-nitroaniline (2.03 g, 12.2 mmol, 1 eq.) was added before sealing and purging with argon. The solid was dissolved in dry dichloromethane (40 mL) giving a clear orange solution and then 4-butylphenyl isocyanate (2.2 mL, 12.5 mmol, 1.02 eq.) was added dropwise under stirring at 40 °C for 24 hours. A precipitate corresponding to the formation of urea **4** was observed. The turbid yellow reaction mixture was filtered and washed with cold ethyl acetate and dried under vacuum to yield pure compound **4** as a yellowish solid (3.26 g, 9.52 mmol, **78%**).

^{1}H NMR (300 MHz, DMSO-D_6), **Figure S9**, δ (ppm) = 9.06 (s, H_g), 8.71 (s, H_l), 8.13 (s, H_h), 7.36 (d, J = 8.3 Hz, $2H_f$), 7.30 (s, H_j), 7.11 (d, J = 8.3 Hz, $2H_e$), 2.50 (m, $2H_d$), 2.45 (s, $3H_k$), 2.30 (s, $3H_i$) 1.53 (qt, J = 7.5 Hz, $2H_c$), 1.29 (hx, J = 7.5 Hz, $2H_b$), 0.89 (t, J = 7.2 Hz, $3H_a$).

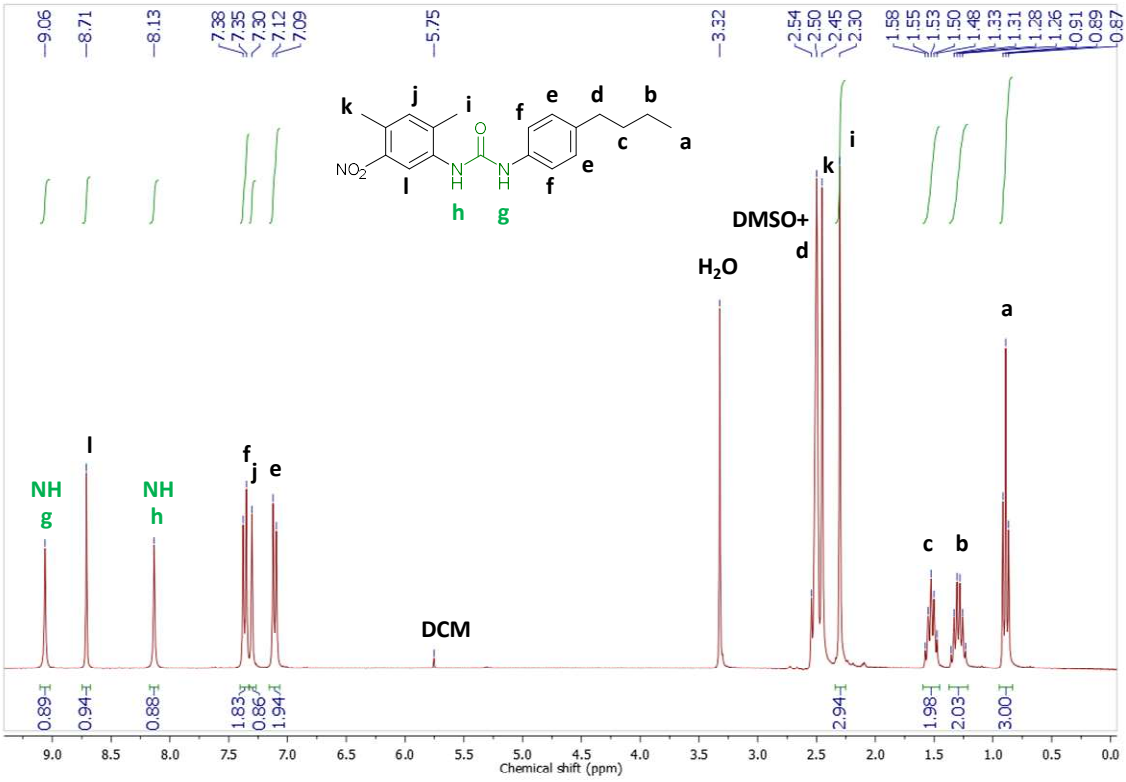

Figure S9. ^{1}H NMR spectrum of **4** in DMSO-D_6

^{13}C NMR (75 MHz, DMSO-D_6), **Figure S10**, δ (ppm) = 152.4, 146.5, 137.0, 136.5, 136.0, 134.1, 132.9**,** 128.6, 126.1, 118.3, 114.9, 34.1, 33.3, 21.7, 19.3, 17.8, 13.8.

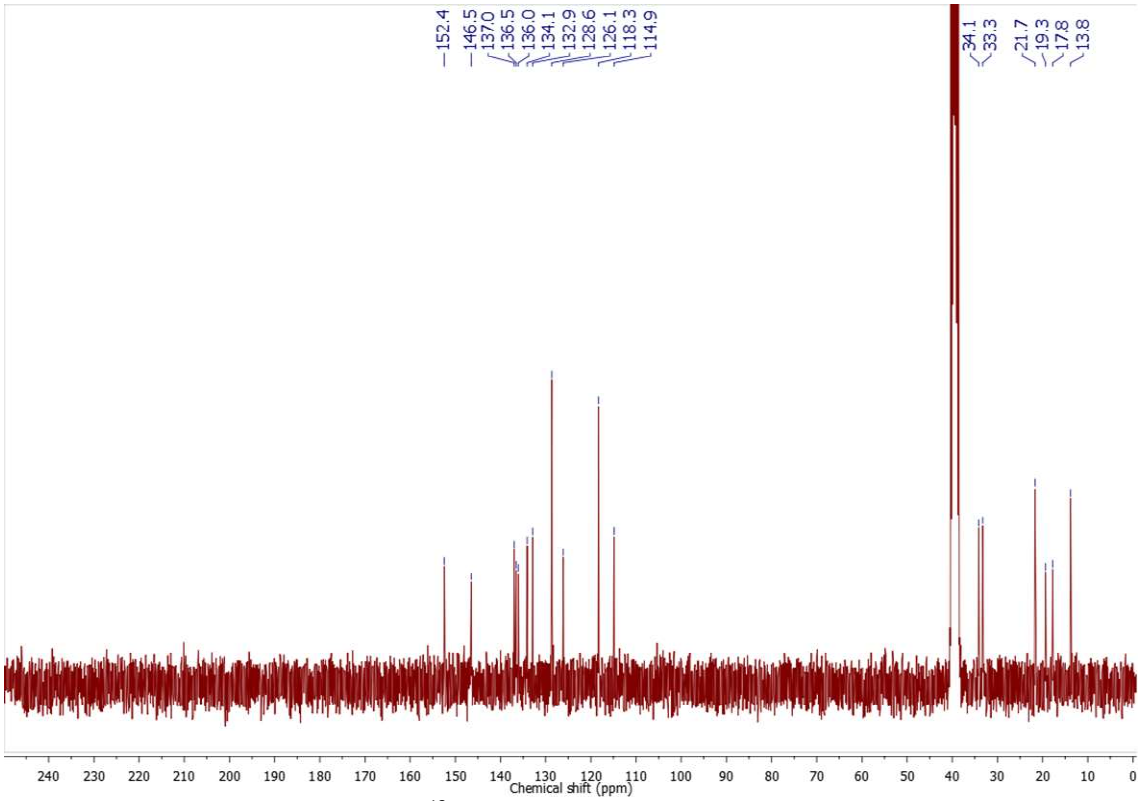

Figure S10. ^{13}C NMR spectrum of **4** in DMSO-D_6

MALDI-TOF MS trans-2-[3-(4-*tert*-Butylphenyl)-2-methyl-2-propenylidene] malononitrile (DCTB):
M_{exp} = 341.4 g/mol, M_{th} = 341.17 g/mol.

EA: theoretical % (C = 66.8, H = 6.8, N = 12.3), experimental % (C = 65.6, H = 6.7, N = 12.1).

m.p. 187-188 °C.

Synthesis of 1-(5-amino-2,4-dimethylphenyl)-3-(4-butylphenyl) (5):

The nitro group of **4** was reduced to an amino group by catalytic hydrogenation in the presence of palladium/carbon according to a procedure described by Tanatani *et al*.[4]

In a 250 mL three-necked round bottom flask, **4** (2.04 g, 6.0 mmol, 1 eq.) and 10% Pd on carbon (0.35 g, 0.33 mmol, 0.05 eq.) were dissolved in a 1/1 mixture of dry tetrahydrofuran and methanol (140 mL). The reaction mixture was first purged with nitrogen before stirring for 4 h at 40 °C under hydrogen atmosphere and then filtered on dicalite. The solvent was removed *in vacuo* to give **5** (1.75 g, 5.6 mmol, **94%**) as a white powder.

^{1}H NMR (300 MHz, DMSO-D_6), **Figure S11**, δ (ppm) = 8.77 (s, H_g), 7.58 (s, H_h), 7.34 (d, J = 8.4 Hz, $2H_f$), 7.14 (s, H_l), 7.07 (d, J = 8.4 Hz, $2H_e$), 6.68 (s, H_j), 4.59 (s, $2H_m$), 2.50 (m, $2H_d$), 2.05 (s, $3H_i$), 1.97 (s, $3H_k$), 1.52 (qt, J = 7.5 Hz, $2H_c$), 1.29 (hx, J = 7.5 Hz, $2H_b$), 0.89 (t, J = 7.2 Hz, $3H_a$).

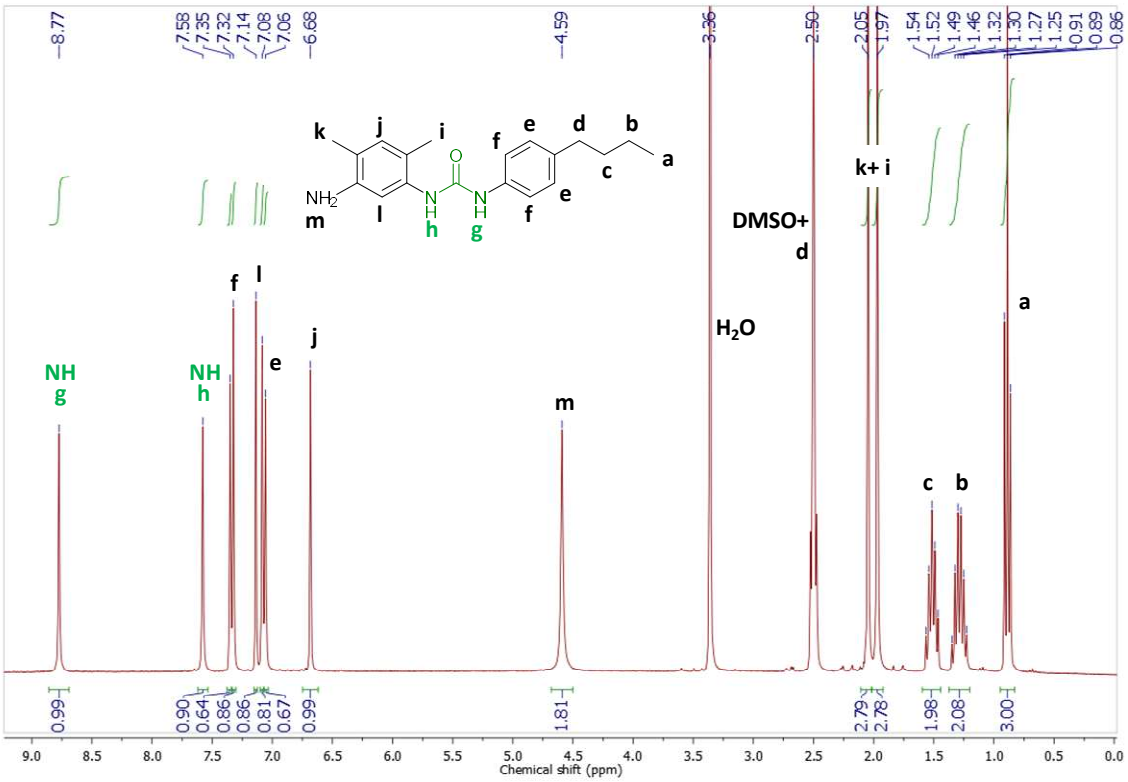

Figure S11. ^{1}H NMR spectrum of **5** in DMSO-D_6

^{13}C NMR (75 MHz, DMSO-D_6), **Figure S12**, δ (ppm) = 152.7, 144.5, 137.8, 135.4, 135.3, 131.4, 128.6, 117.9, 115.9, 114.9, 107.8, 34.2, 33.4, 21.7, 16.9, 16.8, 13.9.

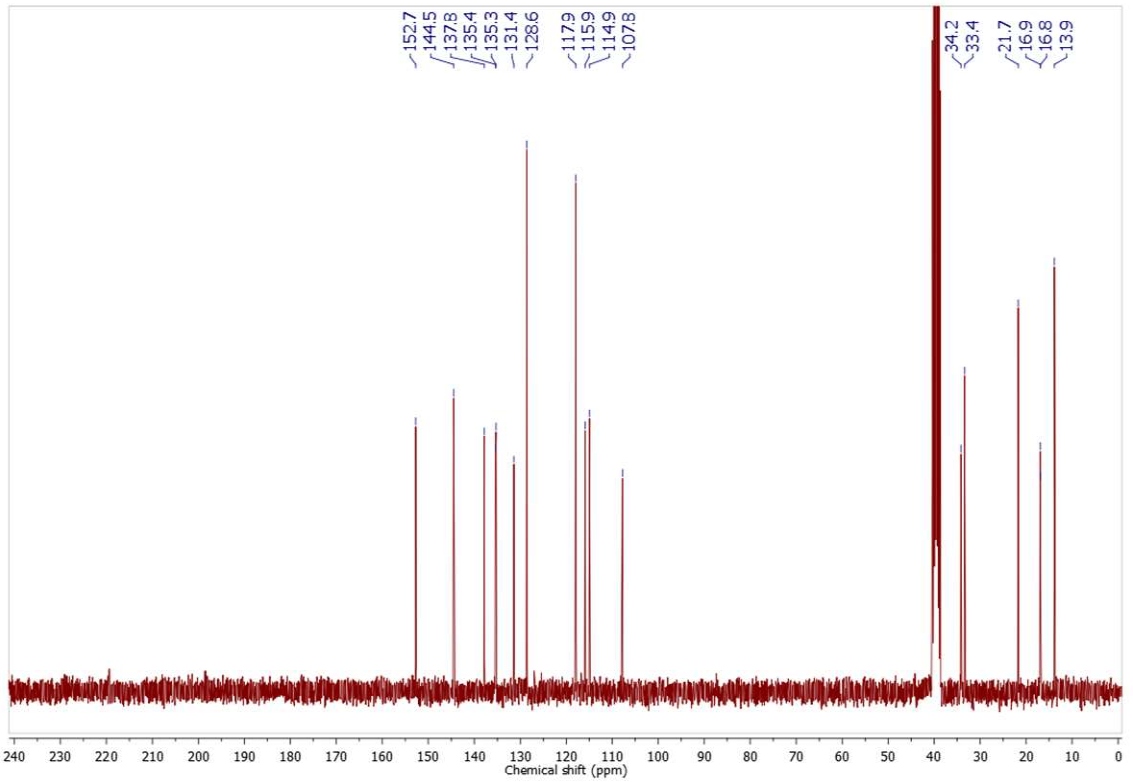

Figure S12. ^{13}C NMR spectrum of **5** in DMSO-D_6

DSQ: M_{exp} = 311.00 g/mol, M_{th} = 311.20 g/mol.

EA: theoretical % (C = 73.3, H = 8.1, N = 13.5), experimental % (C = 73.1, H = 8.1, N = 13.3).

Synthesis of PEO-NDI-U_2:

Compound **5** was converted into an isocyanate group using triphosgene in the presence of N,N-diisopropylethylamine according to a procedure described by Bouteiller *et al*.[5] The isocyanate intermediate was not isolated and *in situ* reacted with **3** leading to the targeted **PEO-NDI-U_2** polymer.

Compound **5** (0.0375 g, 0.12 mmol, 1 eq.) and *N,N*-diisopropylethylamine (23 µL, 0.13 mmol, 1.1 eq.) were dissolved in dry THF (250 µL) under argon. This solution was subsequently transferred via a syringe within five minutes to a solution of triphosgene (0.0135 g, 0.05 mmol, 0.38 eq.) in dry THF (0.3 mL) under argon. After three hours, a solution of **3** (0.233 g, 0.11 mmol, 0.88 eq.) and *N,N*-diisopropylethylamine (44 µL, 0.25 mmol, 2.4 eq.) in dry THF (0.8 mL) was added quickly via a double-tipped syringe and let overnight under stirring. FT-IR confirmed the disappearance of the isocyanate function (≈2270 cm^{-1}). The reaction mixture was concentrated under reduced pressure, precipitated in ice-cold ethanol, filtered on a sintered funnel and rinsed with cold ethanol and pentane yielding **PEO-U_2-NDI** (0.140 g, 0.06 mmol, **58%**) as a brown powder.

Molecular characteristics (molar masses and dispersity (Đ)) were estimated by ^{1}H NMR, MALDI-TOF and SEC in DMF + LiBr (see **Table S1**).

Table S1. Molecular characteristics of **PEO-NDI-U_2** with a theoretical M_n = 2560 g/mol for a PEO arm with a polymerization degree DP_n = 42.

	MALDI	RMN	SEC[a]
M_n (g/mol)	2510	2770	3870
M_w (g/mol)	2530	/	4050
Đ	1.01	/	1.05

[a] Measured in DMF + LiBr in PMMA-equivalents

^{1}H NMR (400 MHz, $CDCl_3$), **Figure S13**, δ (ppm) = 8.70-8.58 (m, $4H_q + H_g$), 7.78 (s, H_l), 7.64 (s, H_h), 7.50 (s, H_m),7.26 (d, J = 8.5 Hz, $2H_f$), 7.04 (d, J = 8.5 Hz, $2H_e$), 6.84 (s, H_j), 6.39 (t, J = 6 Hz, H_n),4.30-4.10 (m, $2H_p + 2H_r$), 3.70-3.30 (m, 200H ~ $2H_t \times DP_n + 2H_u \times DP_n + 2H_o + 2H_s$), 3.24 (s, $3H_v$), 2.50 (m, $2H_d$), 2.08 (s, $3H_i$), 1.97 (s, $3H_k$), 1.52 (qt, J = 7.5 Hz, $2H_c$), 1.30 (hx, J = 7.5 Hz, $2H_b$), 0.90 (t, J = 7.3 Hz, $3H_a$).

The integral value corresponding to the protons of the polymer is not exactly the same for the molecules **PEO-NDI**, **2**, **3** and **PEO-NDI-U_2** but correspond within experimental error to a polymerization degree DP_n ~ 42.

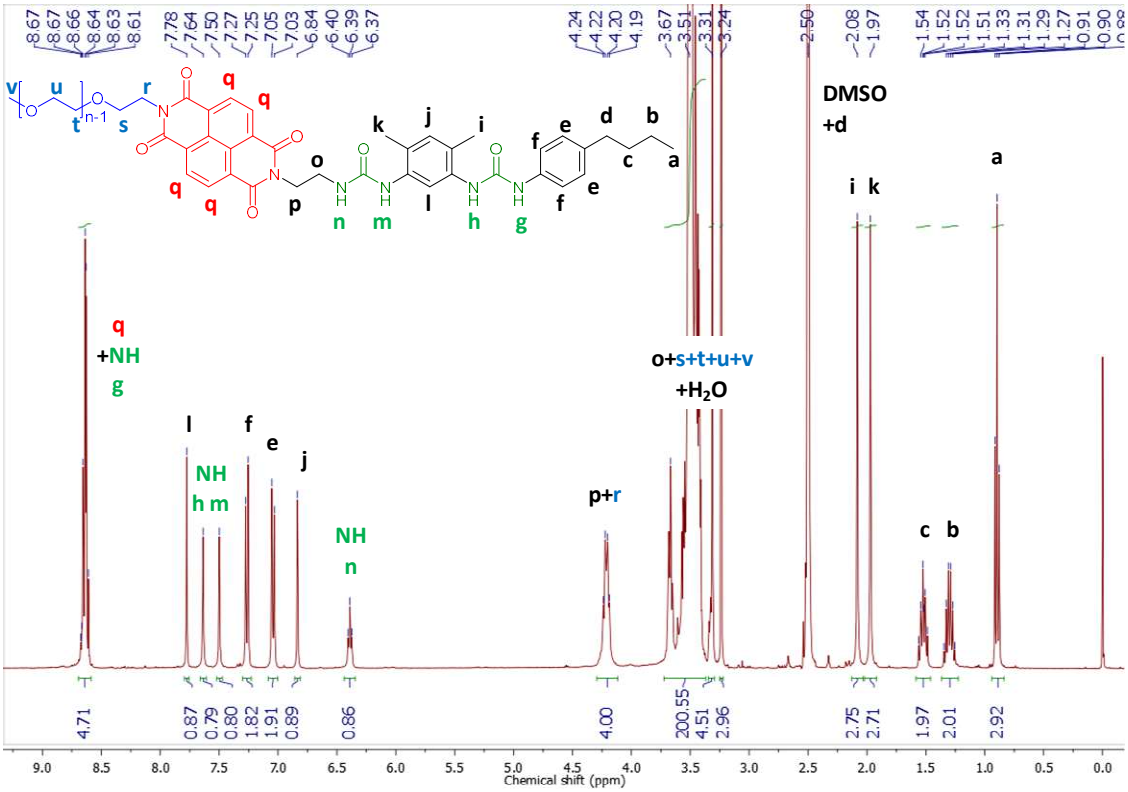

Figure S13. ^{1}H NMR spectrum of **PEO-NDI-U$_2$** in DMSO-D$_6$

MALDI-TOF MS (2-(4-hydroxybenzeneazo)benzoic acid (HABA), Na^+):

M_{exp} (for n = 42) = 2532.20 g/mol, M_{th} (for n = 42) = 2532.35 g/mol. Details are given in **Figure S14**.

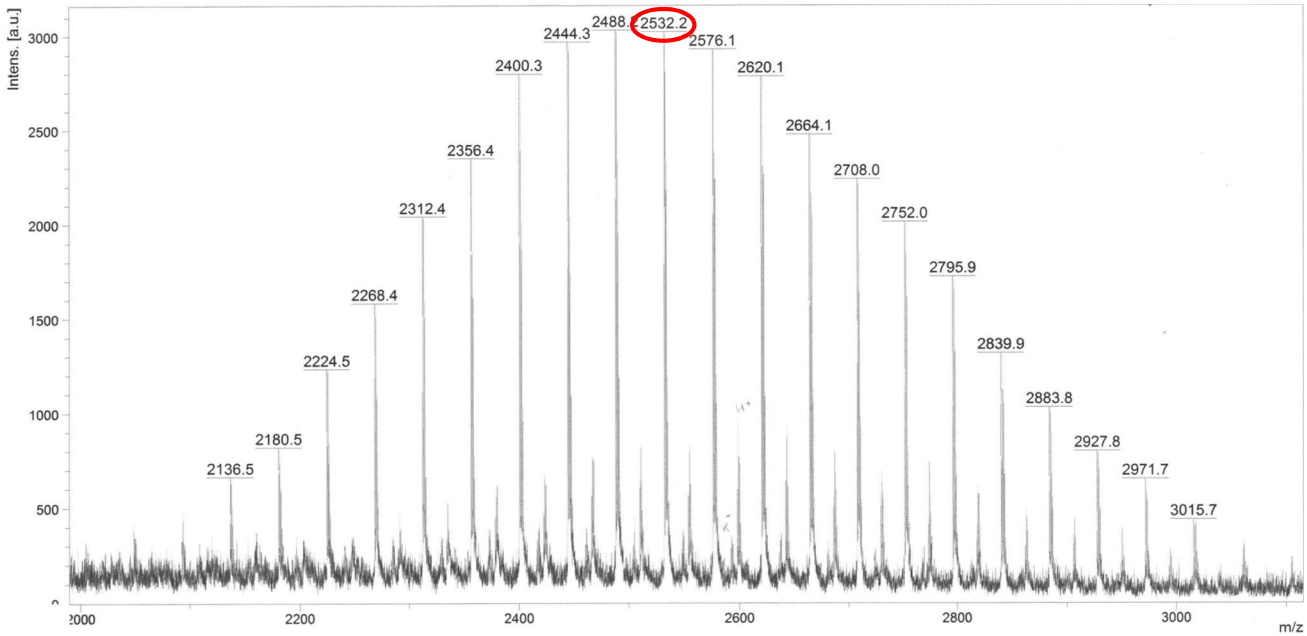

Figure S14. MALDI-TOF of **PEO-NDI-U$_2$** with 2-(4-hydroxybenzeneazo)benzoic acid used as matrix without salt addition

SEC (calibration: PMMA): $M_n = 3.9 \times 10^3$ g/mol, $M_w/M_n = 1.05$, is given in **Figure S15**.

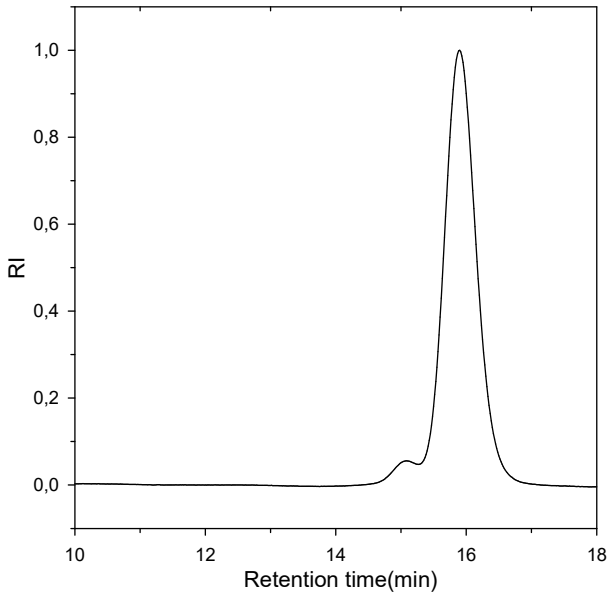

Figure S15. SEC chromatogram of **PEO-NDI-U_2** solution in DMF/LiBr

2 Characterization of the self-assembly in solution

2.1 Material

Cryo transmission electron microscopy (cryoTEM) was carried out on a 2100 HR microscope (Jeol) running at 120 kV equipped with a LaB_6 filament. Specimens for cryoTEM observations were treated using a cryo-plunge 3 system (Gatan) in which a drop of the aqueous solution was deposited onto glow-discharged carbon-coated grids (Agar Scientific). The TEM grid was then blotted so that a thin liquid layer was formed spanning across the holes of the supporting carbon film. The grid was quickly plunged into liquid ethane cooled by liquid nitrogen to vitrify the liquid film. The vitrified specimens were put in a cryo-transfer specimen holder (626, Gatan) cooled with liquid nitrogen. The samples were observed at −176 °C and recorded with a 2048 × 2048 ORIUS SC200D CCD camera (Gatan). **Figure 1** was treated with the software Fiji.

UV-Vis absorption spectra were recorded on a Jasco V760 spectrometer using a quartz cuvette with a path length of 10 mm at room temperature.

Light scattering measurements were done with a standard ALV-CGS3 system equipped with an ALV-5003 multi tau correlator system (ALV GmbH, Germany) with a vertically polarized helium-neon laser with wavelength λ = 633 nm as light source. The measurements were done at 20 °C over a large range of scattering wave vectors q varying from ca. 2.8×10^{-4} Å^{-1} to 2.6×10^{-3} Å^{-1} including low and high limit for the solvents used. $q = \frac{4\pi n}{\lambda}\sin\left(\frac{\theta}{2}\right)$, with θ the angle of observation, n the refractive index of the solvent and λ = 633 nm the wavelength of the laser. The apparent hydrodynamic radius was determined by dynamic light scattering and the apparent radius of gyration and molecular weight were determined by static light scattering. Note that it was verified that in the concentration-range investigated, the absorbance of the solutions at 633 nm was negligible for all samples according to UV/vis spectroscopy, making these solutions suitable for LS measurement.
PEO-NDI-U$_2$ and **PEO-NDI** were observed by fluorescence spectroscopy on a Fluoromax-4 apparatus to emit weakly upon photoexcitation at 633 nm (data not shown); which could have affected the LS results. LS measurements were therefore first compared with and without an optical filter (Edmund Optics 65711 632NM 1-46-17, central wavelength (CWL) bandpass filter = 632 nm, bandwidth (FWHM) = 10 nm) for each polymer in the different solvents investigated. For both **PEO-NDI** and **PEO-NDI-U$_2$**, no significant difference was observed, implying that the contribution of fluorescence to the detected light could be neglected. Experiments were then mostly conducted without any optical filter.

Static light scattering (SLS) treatment

The absolute intensity, I in cm^{-1}, scattered by the polymer was determined according to **(Equation S1)**.

$$\mathrm{I} = \frac{I_{solution}(\theta) - I_{solvant}(\theta)}{I_{toluene}(\theta)} \times \left(\frac{n_{solvent}}{n_{toluene}}\right)^2 \times R_{toluene} \qquad \textbf{(Equation S1)}$$

With $I_{solution}$, $I_{solvent}$ and $I_{toluene}$ the average intensities scattered, respectively, by the solution, the solvent, and the reference (toluene) at angle θ; $n_{solvent}$ = 1.33 for water and D_2O, 1.33 for methanol, 1.34 for acetonitrile and $n_{toluene}$ = 1.496 correspond to the respective refractive indexes of the solvents and of toluene; and $R_{toluene} = 1.35 \times 10^{-5}$ cm^{-1} the Rayleigh ratio of toluene for a wavelength λ = 633 nm. For water/DMSO (99/1) solutions, $n_{solvent}$ was taken equal to n_{water}.

Dynamic Light Scattering (DLS)

The normalized electric field autocorrelation functions ($g_1(t)$) obtained by DLS measurements were analyzed in terms of a relaxation time (τ) distribution: $g_1(t) = \int A(\tau) e^{\left(\frac{-t}{\tau}\right)} d\tau$.

PEO-NDI-U$_2$

For all **PEO-NDI-U$_2$** solutions in water, acetonitrile or methanol, only one q^2-dependent relaxation mode was observed. The REPES routine was mainly used to obtain $A(\tau)$ without assuming a specific shape for the distribution.[6] $A(\tau)$ was also determined for **Figure S20** using the GAUSS routine that assumes a log-normal distribution of relaxation times because it allows a more precise estimation of the dispersity of relaxation times (and therefore of R_h).

The apparent diffusion coefficient D was calculated from the average relaxation rate of this relaxation mode as $D = \langle \tau^{-1} \rangle / q^2$. D is related to the apparent hydrodynamic radius, R_{app}, of the solute according to **(Equation S2**.

$$R_{app} = \frac{k_B T}{6\pi\eta D} \qquad \textbf{(Equation S2)}$$

With k Boltzmann's constant, T the absolute temperature and η the viscosity of the solvent.

When the particles are small compared to q^{-1} and the solutions are sufficiently dilute so that interactions can be neglected, R_{app} is equal to the z-average hydrodynamic radius, R_h.

(Equation S3 was used in order to estimate the length of the cylinders formed by **PEO-NDI-U$_2$** in aqueous medium from R_h assuming that the cylinders are rigid.[7,8]

$$R_h = \frac{L}{2\sigma - 0.19 - \frac{8.24}{\sigma} + \frac{12}{\sigma^2}} \qquad \textbf{(Equation S3)}$$

With $\sigma = \ln\left(\frac{L}{r}\right)$, L the length of the cylinder and r its cross sectional radius.

PEO-NDI

For **PEO-NDI** in water, two populations of scattering particles were observed by DLS, a slow and a fast one. It was observed that the slow mode of relaxation corresponded to R_{app} values about 10 times as large as those of the fast mode of relaxation ($R_{app,slow} \approx 50$ nm, $R_{app,fast} \approx 5$ nm). As a conclusion, even though the slow mode of relaxation contributed significantly to the DLS and SLS signals because of its large molecular weight, its weight percentage within the sample could be neglected. The SLS and DLS data presented in the manuscript therefore correspond to the contribution of the fast mode of relaxation assuming that the contribution of the slow mode in terms of weight concentration can be neglected. A similar behavior has already been observed in the literature for many other self-assembling systems[9–13] and the same treatment was applied to get rid of the contribution of the large aggregates.

Differential refractometry. The refractive index increment (∂n/∂C) of **PEO-NDI-U_2** was measured in various solvents (λ = 633 nm) using a differential refractometer OpriLab rEX from Wyatt Technology Corporation with the software Astra. The samples at various concentrations were injected at room temperature using a flow rate of 1 mL.min^{-1}. The values obtained were compared to values found in the literature for PEO homopolymer. For comparison a PEO homopolymer (M_n = 2000 g/mol and Đ = 1.1, Aldrich) was also measured in DMSO and toluene. All data are summarized in **Table S2**.

Table S2. ∂n/∂C in mL/g of **PEO-NDI-U_2** and PEO homopolymers in various solvents

Solvents	∂n/∂C (PEO-NDI-U_2)	∂n/∂C (PEO)
Dimethyl sulfoxide	0.021	-0.006[a]
Toluene	0.026	-0.014[a]
Acetonitrile	0.157	0.135[b]
Methanol	n.a.	0.149[c]
Water	0.165	0.139[d]

[a] Measured on a PEO 2000 g/mol, [b-d] values found in the literature for PEO homopolymers:[14] [b] M_w = 9400 g/mol, λ = 546 nm, [c] M_w = 3000 g/mol, λ = 546 nm, [d] M_w = 6000 g/mol, λ = 546 nm.

Small angle neutron scattering (SANS) measurements were made at Laboratory Léon Brillouin (LLB Saclay France) on device PA20 (G 5.1) at a constant wavelength λ = 6 Å and for three sample-detector distances (1.1, 8 and 17.5 m) covering a 2 × 10^{-3}-0.3 Å^{-1} q-range. The scattering vector q is defined assuming elastic scattering as $q = \frac{4\pi}{\lambda}\sin\left(\frac{\theta}{2}\right)$ with θ the angle between the incident and the scattered beam. Solutions were measured in Hellma cylindrical cells with an optical path length of 2 mm and a volume of 560 µL. Data were processed with Pasinet Software (http://www-llb.cea.fr/Phocea/Page/index.php?id=84), corrected for transmission and thickness. The empty cell signal, the solvent, the electronic noise and the incoherent background were substracted. A light water standard was used to normalize the scattering intensities to cm^{-1} units.

2.2 Preparation of the solutions for light and neutron scattering experiments

For neutron scattering experiments, only deuterated solvents were used in order to maximize the contrast and have a reasonable acquisition time. For light scattering, solutions were prepared using Millipore water (deionized water, resistivity > 18 MΩ.cm) and/or analytical grade organic solvents. Some samples measured by SANS in D_2O were also studied by LS confirming the negligible difference of self-assembly of PEO-U_2-NDI in D_2O compared to H_2O.

Direct dispersion (in pure solvents). For solutions prepared in a single solvent (water, methanol, acetonitrile, toluene and corresponding deuterated solvents), the polymer was directly dispersed in the pure solvent at the desired concentration and stirred at least overnight at room temperature unless specified otherwise.

Dispersion in water-DMSO mixtures (according to Han *et al.*[13]). Here, the polymer was first dissolved in pure DMSO (resp. DMSO-D_6 for SANS) at 100 g/L. After stirring for a few minutes, water (resp. D_2O) was added either manually (dropwise over a few minutes) or at a controlled rate of 0.5 mL/h using a syringe pump under stirring to reach a water/DMSO ratio of 99/1 by volume and a polymer concentration of 1 g/L.

The solutions studied by light scattering were filtered over 0.45 µm GHP Acrodisc filters before measurement and it was verified by UV-Vis spectroscopy that the amount of polymer lost during filtration could be neglected.

2.3 Fitting models

2.3.1 Combining SLS and SANS data

The absolute intensity I obtained both from SLS and SANS experiments is related to their concentration C in g.cm^{-3}, to a contrast factor K, to the apparent weight average molecular weight of the scatterers extrapolated to q → 0, M_{app}, and to their form factor P(q), which depends on their shape and size (see below).[15] Note that the apparent molecular weight M_{app} corresponds to the true molecular weight M_w only in very dilute solutions where the interactions between the scatterers can be neglected.[15]

$$I = K.C.M_{app} \times P(q) \qquad \textbf{(Equation S4)}$$

For SLS, $K_{SLS} = \frac{4\pi^2 {n_{solvent}}^2}{\lambda^4 N_a} \times \left(\frac{\partial n}{\partial C}\right)^2$ **(Equation S5)**

Where N_a is Avogadro's number and $\frac{\partial n}{\partial C}$ is the refractive index increment of the polymer in the solvent (see **Table S2**).

For SANS, $K_{SANS} = \frac{\overline{\Delta b}^2}{N_a}$ **(Equation S6)**

where $\overline{\Delta b} = b_2 - \rho_2/d_2$ is the specific contrast of the polymer in the solvent with b_2 the specific scattering length of the polymer (cm.g^{-1}), d_2 is its specific gravity (g.cm^{-3}), and ρ_s is the scattering length per unit volume of the solvent (cm.cm^{-3}). For **PEO-NDI-U$_2$** in D_2O or in D_2O/DMSO-D_6 (99/1), $\overline{\Delta b}^2$, was calculated based on the molecular formula of **PEO-NDI-U$_2$** and using the specific gravity of PEO (d_2 = 1.15 g.cm^{-3}). The value was the same for both solvents ($\overline{\Delta b}^2$ = 2.07 × 10^{21} cm^2.g^{-2}) and yielded K_{SANS} = 3.43 × 10^{-3} mol.cm^2.g^{-2}. In toluene-D_8,, $\overline{\Delta b}^2$ = 1.55 × 10^{21} cm^2.g^{-2} and yielded K_{SANS} = 2.57 × 10^{-3} mol.cm^2.g^{-2}.

PEO-NDI-U$_2$ was prepared at 1 g/L in D_2O/DMSO-D_6 (99/1) using a syringe pump for the addition of water to the concentrated DMSO-D_6 solution (see section 2.2). The same solution was measured both by SLS and SANS. According to **(Equation S4**, $\frac{I_{SLS}}{K_{SLS}.C} = M_{app}.P(q) = \frac{I_{SANS}}{K_{SANS}.C}$. Both SLS and SANS data should therefore superimpose within experimental error by representing $\frac{I}{K.C}$ = f(q) for both sets of data with K_{SLS} = 1.97 × 10^{-7} mol.cm^2.g^{-2} (**Equation S5**) and K_{SANS} = 3.43 × 10^{-3} mol.cm^2.g^{-2} (**Equation S6**). In spite of the fact that the measurement was done with the same solution on both apparatuses, a discrepancy of ~ 35% between $\frac{I_{SLS}}{K_{SLS}.C}$ and $\frac{I_{SANS}}{K_{SANS}.C}$ was observed at q ≈ 2 × 10^{-3} Å that both techniques can access. This difference was mainly attributed to the probable error made on the calculation of K_{SANS} using ρ_{PEO} instead of $\rho_{PEO\text{-}NDI\text{-}U2}$, the latter value being unknown. Considering additionally that the experimental error generally admitted for SANS and SLS is 10-20%, the discrepancy was considered reasonable between the two techniques. The SANS data were therefore slightly corrected to allow proper superposition with the SLS ones. Fitting models were simultaneously applied to the combined SLS and SANS data whenever both were available (see section 2.3.2.).

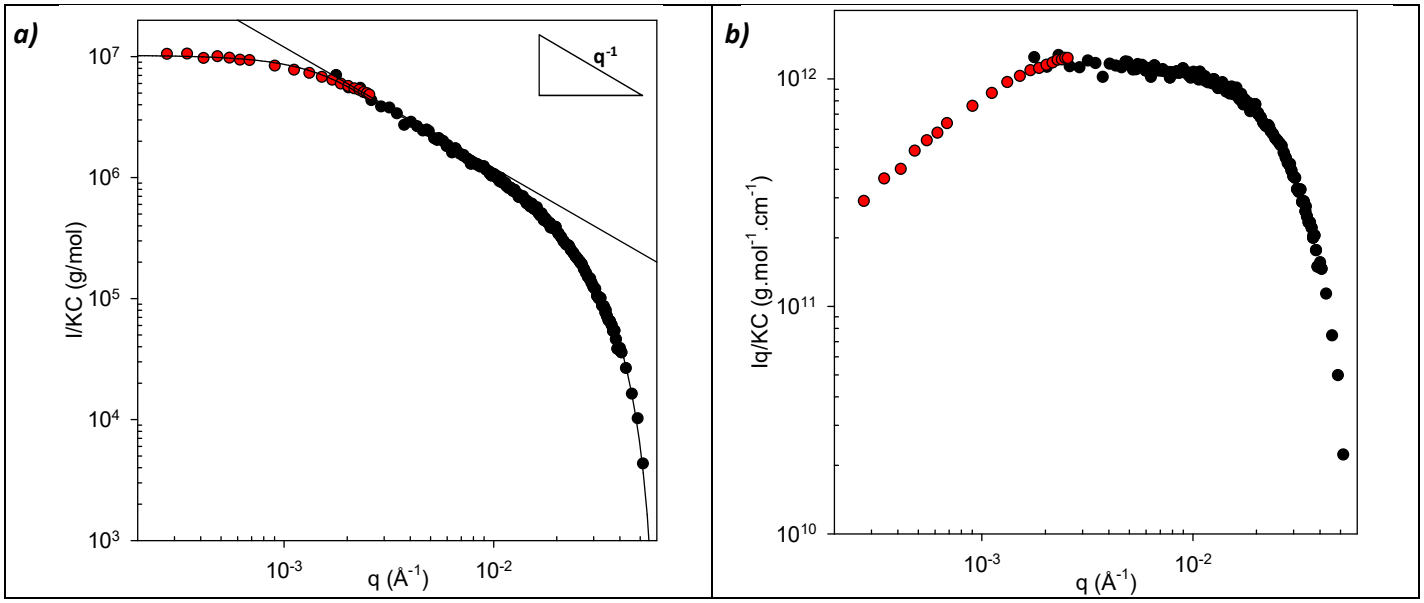

Figure S16. ***a)*** Evolution of I/KC as a function of the scattering wave vector q for SLS (●) and SANS (●) data for **PEO-NDI-U$_2$** at 1 g/L in D_2O/DMSO-D_6 (99/1) with a syringe pump (this figure corresponds to **Figure 2** in the manuscript). Fitting was done with a model of monodisperse homogeneous cylinders (▬, $M_w = 10^7$ g/mol, r = 6.5 nm, L = 255 nm), ***b)*** Iq/KC as a function of the scattering wave vector (q)

PEO-NDI-U$_2$ was also prepared by direct dispersion, respectively at 1 g/L in H_2O for SLS and at 10 g/L in D_2O for SANS. However, at 10 g/L in D_2O, repulsive interactions between the scatterers are clearly visible as revealed by comparing those data with the data obtained at 1 g/L in D_2O/DMSO-D_6 99/1 vol/vol (**Figure S17**). Because of these interactions, the data obtained by SANS in D_2O at 10 g/L could not be superimposed with the data obtained at 1 g/L in H_2O by SANS. Nevertheless, at the largest q values where repulsive interactions do not play a role anymore, the SANS data at 10 g/L in D_2O and at 1 g/L in D_2O/DMSO-D_6 99/1 vol/vol are perfectly consistent.

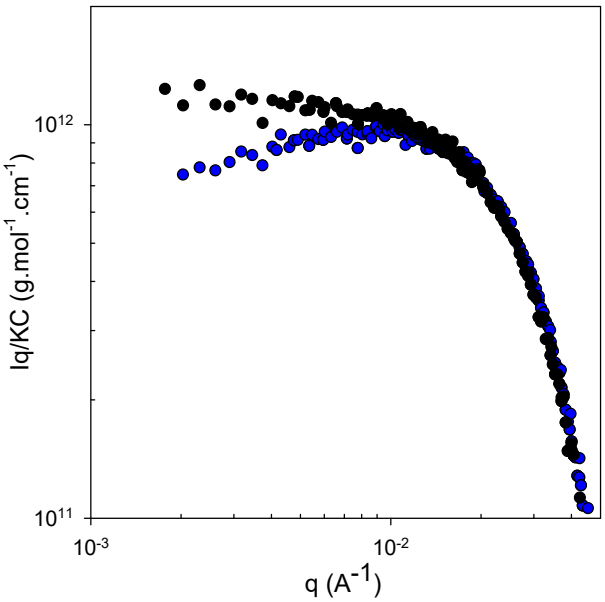

Figure S17. Comparison of Iq/KC as a function of the scattering wave vector q for **PEO-NDI-U2** at 10 g/L in D_2O (●) or at 1 g/L in D_2O/DMSO-D_6 99/1 (vol/vol) (●) obtained by SANS. Both sets of data were corrected with the correction factor between SLS and SANS determined with the latter solution.

2.3.2 Models

Guinier model.

The apparent radius of gyration R_g of **PEO-NDI-U$_2$** assemblies could be determined with a Guinier model[15] (**Equation S7**) which fitted the data only at the lowest q values where $q.R_g < 1$ (Fit not shown).

$$P(q) = e^{\left(-\frac{q^2 \times {R_g}^2}{3}\right)} \quad \textbf{(Equation S7)}$$

Model of cylinders.

a) Fitting over the whole q-range

The SLS and SANS data obtained for solutions of **PEO-NDI-U$_2$** at 1 g/L in D_2O/DMSO 99/1 (vol/vol) were fitted using a model of homogeneous cylinders with uniform contrast[15,16] using the open source SASView Software (http://www.sasview.org/). For the model of monodisperse cylinders presented in the manuscript (**Figure 2**), the adjusted parameters were the length L of the cylinders, their weight average apparent molar mass M_{app} and their cross sectional radius r.

b) Determination of the radius of the cylinders and of the molecular weight per Å

When the cylinders are very long, the model of homogenous cylinders used in SASView can be simplified into **(Equation S8)** valid for infinitely long cylinders.[17,18]

$$I = \frac{\pi C}{q}.\mathrm{K}.M_L\left[2\frac{J_1(qr)}{qr}\right]^2 \quad \textbf{(Equation S8)}$$

$$(qI)_{q\to 0} = (qI)_0 \exp\left(-\frac{\mathrm{r}^2}{4}q^2\right) \quad \textbf{(Equation S9)}$$

$$(qI)_0 = \pi C.\mathrm{K}.M_L \quad \textbf{(Equation S10)}$$

Where C is the polymer concentration (g.cm^{-3}), M_L is the molecular weight per unit length of the cylinder (g.mol^{-1}.cm^{-1}), r is the radius of the cross section, K is the contrast defined as in **(Equation S5)**,(**Equation S6)** and J_1 is the Bessel function of first kind.

These equations where successfully applied to fit the q-range where I.q is constant (that is I is q^{-1}-dependent) yielding the radius of the cross-section of the cylinders and the molecular weight per unit of length.

c) Determination of the number of molecules within the cross section of the cylinders by SLS and SANS

Two consecutive ureas interacting through hydrogen bonds in a 1D structure are separated by an intermolecular distance of 0.46 nm.[19] If the **PEO-NDI-U$_2$** were stacked one on top of the other with only one molecule within the cross-section of the cylinder, M_L should be equal to $M_{L(stack)} = M_w$ unimer/0.46 ≈ 6000 g.mol^{-1}.nm^{-1}. However, as described in **Figure S16.*b)***, we found $\frac{I.q}{KC} = 1.1 \times 10^{12} g.mol^{-1}.cm^{-1}$ leading to M_L ≈ 3.5 × 10^4 g.mol^{-1}.nm^{-1} suggesting that the cross-section within cylinder contains ca. 6 molecules of **PEO-NDI-U$_2$**.

2.4 Characterization of the self-assembly in solution

2.4.1 Influence of the concentration

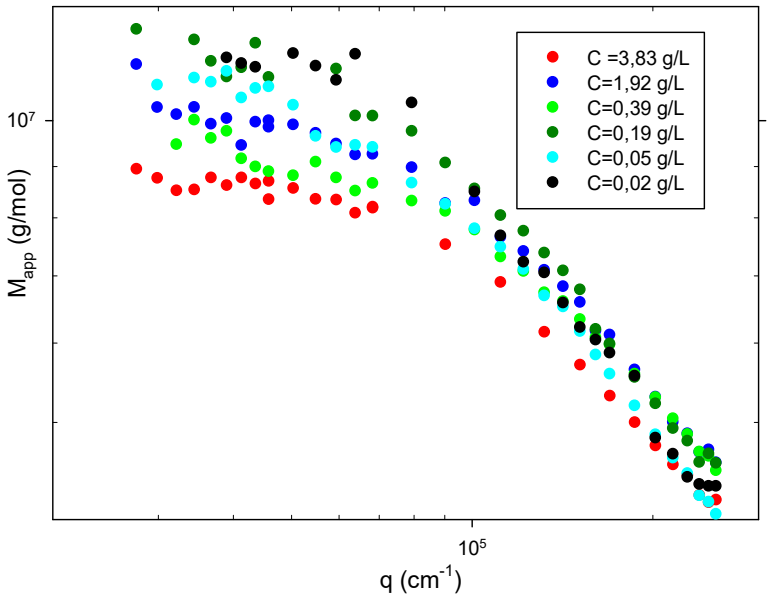

Figure S18. SLS of **PEO-NDI-U$_2$** in water at various concentrations

The self-assembly of **PEO-NDI-U$_2$** in water was studied as a function of concentration from 2×10^{-2} to 3.8 g/L. Between 2×10^{-2} and 2 g/L, the scattered intensity hardly depends on the concentration for $q > 10^5$ cm^{-1}, whereas for $q < 10^5$ cm^{-1}, it does not systematically depend on the polymer concentration. It was concluded that the variation of M_{app} with C in this q-range, which is about 15% maximum, was not due to interactions between the particles (which would have resulted in a systematic variation of M_{app} with C) but to a certain variability in the preparation of the solutions. The latter can potentially be attributed to the formation of out-of-equilibrium structures, the characteristics of which are known to depend on the preparation conditions and to show some lack of reproducibility.[20] Consequently, repulsive interactions between the particles were considered negligible between 2×10^{-2} and 2 g/L, yielding true rather than apparent values of M_w, N_{agg}, L and R_g.

2.4.2 Time and temperature dependence of the self-assemblies

PEO-NDI-U$_2$ was dispersed directly in water and the stability of the resulting self-assemblies was investigated by light scattering. As seen in **Figure S19.*a***, there is no strong evolution observed by SLS at room temperature from 30 to 540 min.

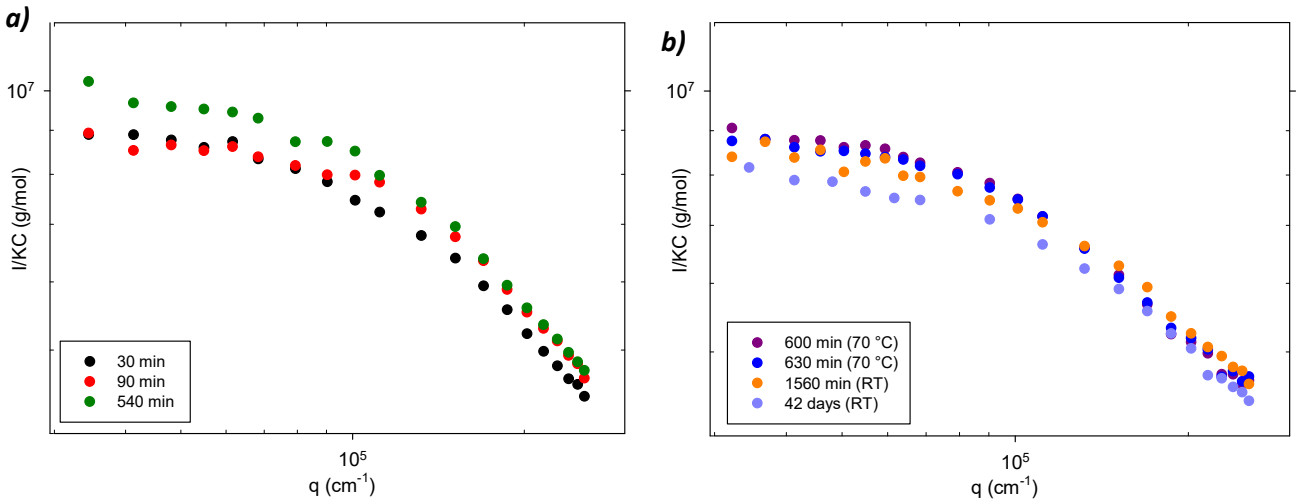

Figure S19. ***a)*** Time- and ***b)*** temperature-dependent evolution of I/KC as a function of the scattering wave vector q in water for **PEO-NDI-U$_2$** at C = 1 g/L

The evolution of the apparent hydrodynamic radius, determined by DLS, reveals a slight decrease of the dispersity of the particles over time with a rather weak time evolution. This is illustrated on **Figure S20.*a*** at a representative observation angle θ = 30° for which the motion of the whole molecule is observed (q.R_h < 1). Investigations were also carried out after one (see **Figure S20.*b***) or several months (data not shown) and no significant change was observed for solutions above 1 g/L. As a conclusion, cylinders of **PEO-NDI-U$_2$** are already present shortly after dispersion of the polymer in water and are very stable over time.

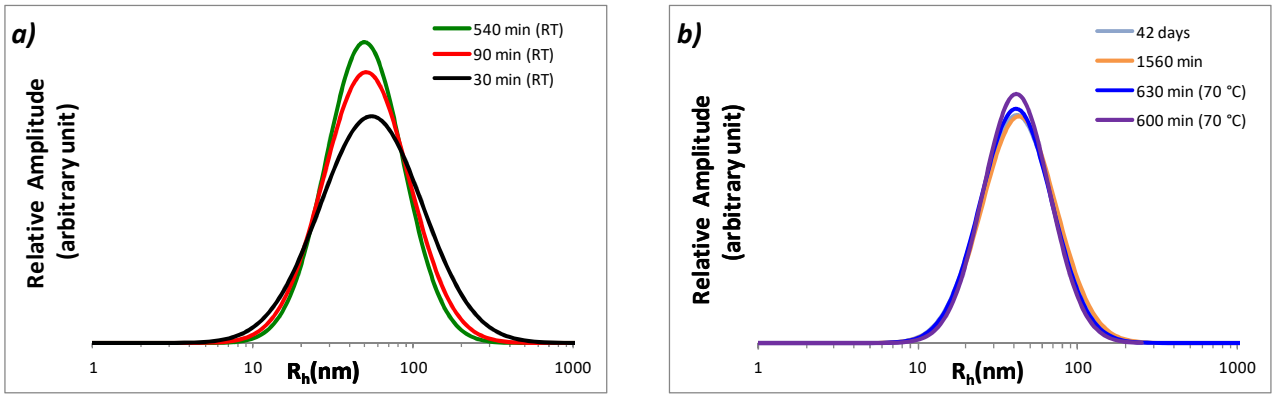

Figure S20. ***a)*** Time- and ***b)*** temperature-dependent evolution of the distribution of apparent R_h obtained by DLS at an observation angle θ = 30° in water for **PEO-NDI-U$_2$** at C = 1 g/L. The raw auto-correlation functions obtained during the DLS measurement were treated using a GAUSS treatment.

After 540 min at 20 °C, the same solutions were heated at 70 °C from 600 to 900 min and measured both directly at 70 °C (after t_0 + 660 min corresponding to 600 min at 20 °C + 60 min at 70 °C) and again at 20 °C at t_0 + 1560 min (**Figure S19.*b*** and **Figure S20.*b***). No significant difference was observed at 20 °C and 70 °C, both by SLS and DLS. The cylinders formed by self-assembly of **PEO-NDI-U$_2$** in water are therefore hardly sensitive to temperature. Note that the variation of dn/dC with temperature was neglected to compare the measurements at 20 and 70 °C because for PEO 14400 g/mol, dn/dC only varies from 0.139 mL/g at 25 °C to 0.115 mL/g at 80 °C for a wavelength of 546 nm.[21]

The impact of temperature on self-assembly was further studied by UV/Vis absorption spectroscopy at 0.25 g/L on a 40-days old solution (**Figure S21**). According to the ratio $I_{0\text{-}0}/I_{0\text{-}1}$ which remains lower than 1, the NDI-NDI interactions

in water stay strong between 20 and 80 °C. The $I_{0\text{-}0}/I_{0\text{-}1}$ ratio even slightly decreased with increasing temperature (**Figure S21** and **Figure S22**), which suggests stronger NDI-NDI interactions.[22]

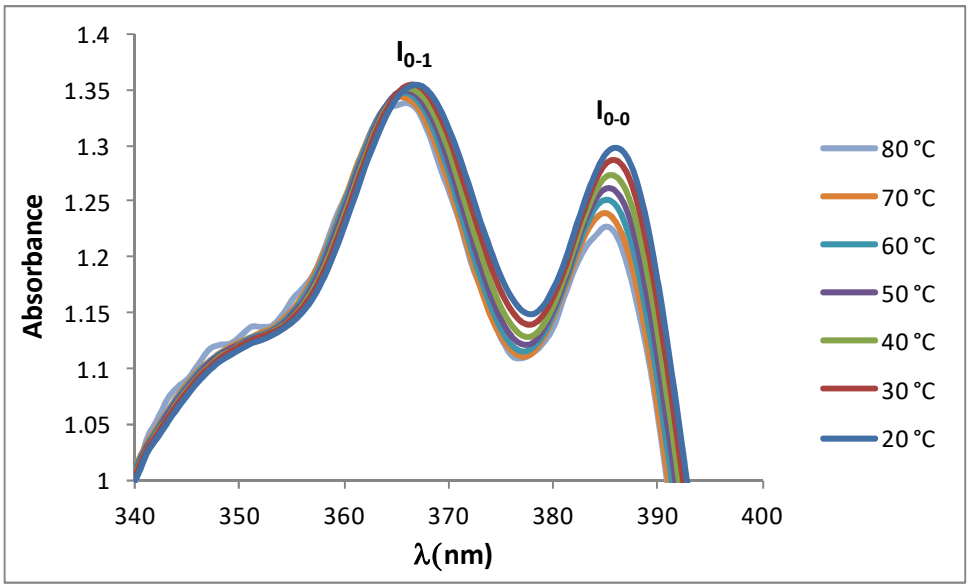

Figure S21. Temperature dependent UV-Vis study of **PEO-NDI-U$_2$** at C = 0.25 g/L in water.

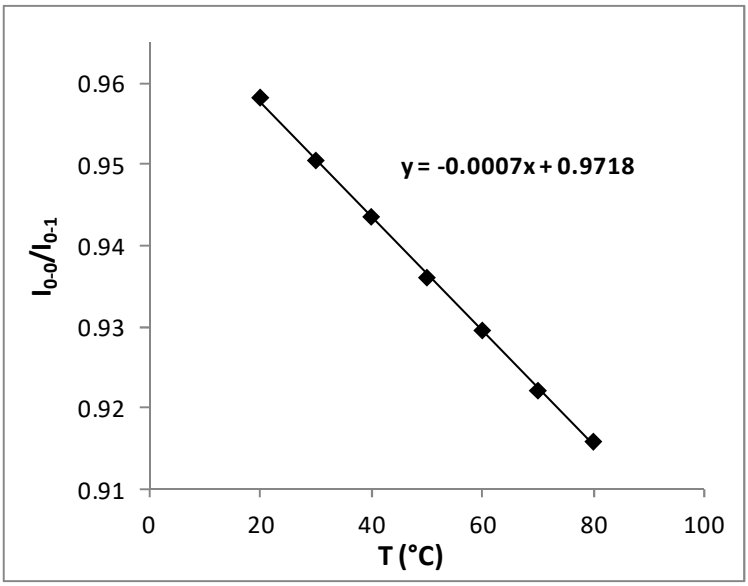

Figure S22. $I_{0\text{-}0}/I_{0\text{-}1}$ ratio as a function of temperature for **PEO-NDI-U$_2$** in water at C = 0.25 g/L

2.4.3 Characterization of PEO-NDI-U_2 in DMSO

2.4.3.a UV-visible absorption spectroscopy

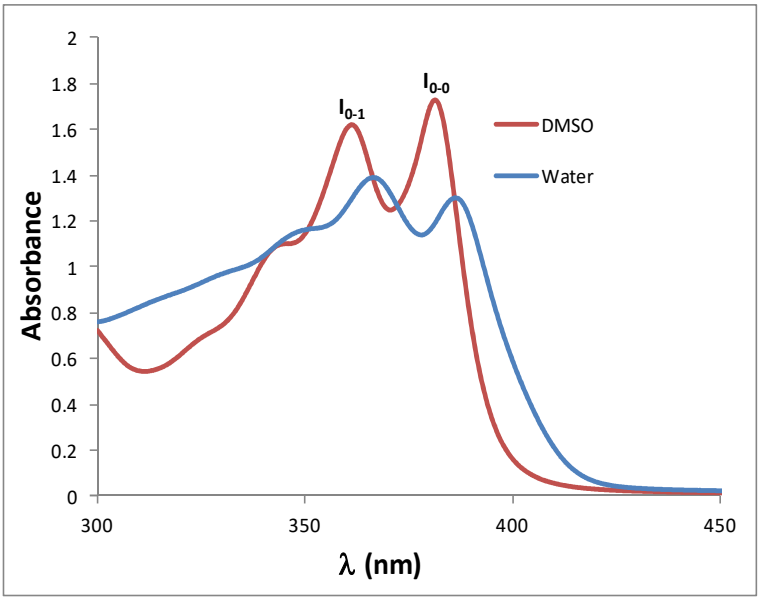

Figure S23. Solvent-dependent UV-visible absorption spectra for **PEO-NDI-U_2** at C = 0.25 g/L (C = 0.1 mM) in DMSO (▬) and water (▬)

The UV-visible absorption spectrum of **PEO-NDI-U_2** in DMSO shows a well-defined absorption band between 300 and 400 nm with two maxima (I_{0-1} and I_{0-0} with respectively λ = 361 and 381 nm) that are characteristic of monomeric NDI chromophore.[22] In water, an inversion of the peak intensity I_{0-1} and I_{0-0} and a bathochromic shift of 5 nm is observed and associated to a face-to-face stacking of NDI units.

2.4.3.b SANS

PEO-NDI-U_2 was studied in DMSO-D_6 by SANS (see **Figure S24**). The data reveal the presence of two sizes of scatterers in solution.

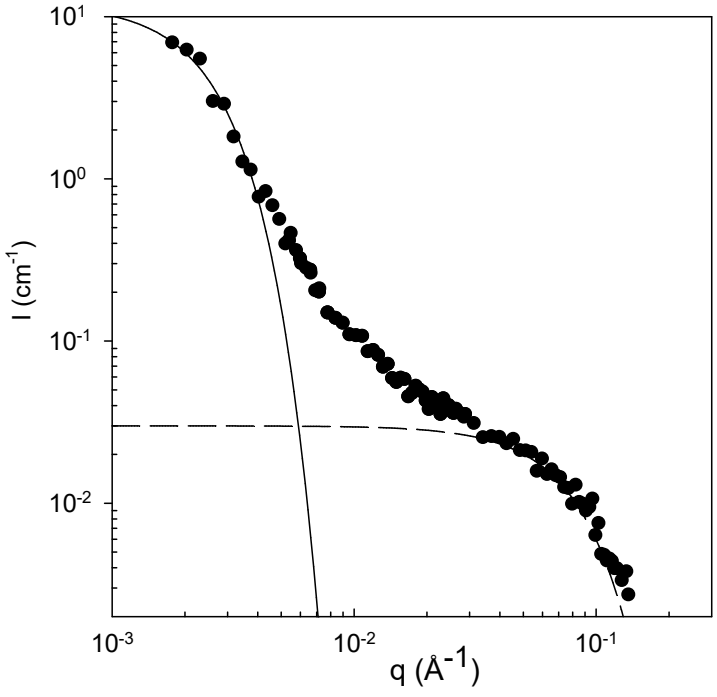

Figure S24. SANS of **PEO-NDI-U_2** in DMSO-D_6 at C = 10 g/L with a Guinier model for the Large (▬) and the small (▪▪▪) populations of scatterers.

The intensity scattered by **PEO-NDI-U$_2$** in DMSO-D_6 at 10 g/L can be described as the contribution of two populations of scatterers (s = small and L = large ones), each following **(Equation S4**. Therefore $I = I_s + I_L$. At q ≈ 10^3 Å, the signal is dominated by the intensity scattered by the large particles for which $P_L(q)$ tends towards 1, so that $I \sim I_L \sim K_L . C_L . M_{app\,L} . P_L(q)$. At q ≈ 10^2 Å, the signal is dominated by the intensity scattered by the small particles for which $P_s(q)$ tends towards 1, so that $I \sim I_s \sim K_s . C_s . M_{app\,s} . P_s(q)$. Assuming that the contrast of both types of particles is similar and that they have the same density, $\frac{I_L}{I_s} = \frac{C_L}{C_s} . \frac{M_{app\,L}}{M_{app\,s}}$ with $M_{app\,L} = \frac{4}{3}\pi\left(R_{gL}\right)^3 . \rho_L . N_a$ and $M_{app\,s} = \frac{4}{3}\pi\left(R_{gs}\right)^3 . \rho_s . N_a$ with R_g, the radius of gyration and N_a, the Avogadro's number). Therefore $\frac{C_L}{C_S} = \frac{\left(R_{gs}\right)^3}{\left(R_{gL}\right)^3} . \frac{I_L}{I_S}$ with R_g estimated using a Guinier model to R_{gs} = 2.2 nm and R_{gL} = 72 nm respectively; leading to $\frac{CL}{C_S} \sim 9 \times 10^{-3}$. In other words, the amount of large particles is negligible in comparison to that of small particles.

The molecular weight corresponding to the small scatterers was therefore calculated using $I_s = 3.10^{-2}$ cm^{-1}, $\overline{\Delta b}^2 = 1.3 \times 10^{21}$ $cm^2.g^{-2}$ and $C_s = C_{total} = 10^{-2}$ $g.cm^{-3}$. We found M_s = 1400 g/mol which is in reasonable agreement with $M_{w\,unimer}$ = 2600 g/mol.

As a conclusion, **PEO-NDI-U$_2$** mainly forms unimers in DMSO.

2.4.3.c DOSY

PEO-NDI-U_2 was studied in DMSO-D_6 at 20 g/L at 25 °C, revealing one single diffusion coefficient D = 0.7 × 10^{-10} $m^2.s^{-1}$, corresponding to R_h ≈ 1.6 nm (see **(Equation S2**) consistent with the formation of unimers.

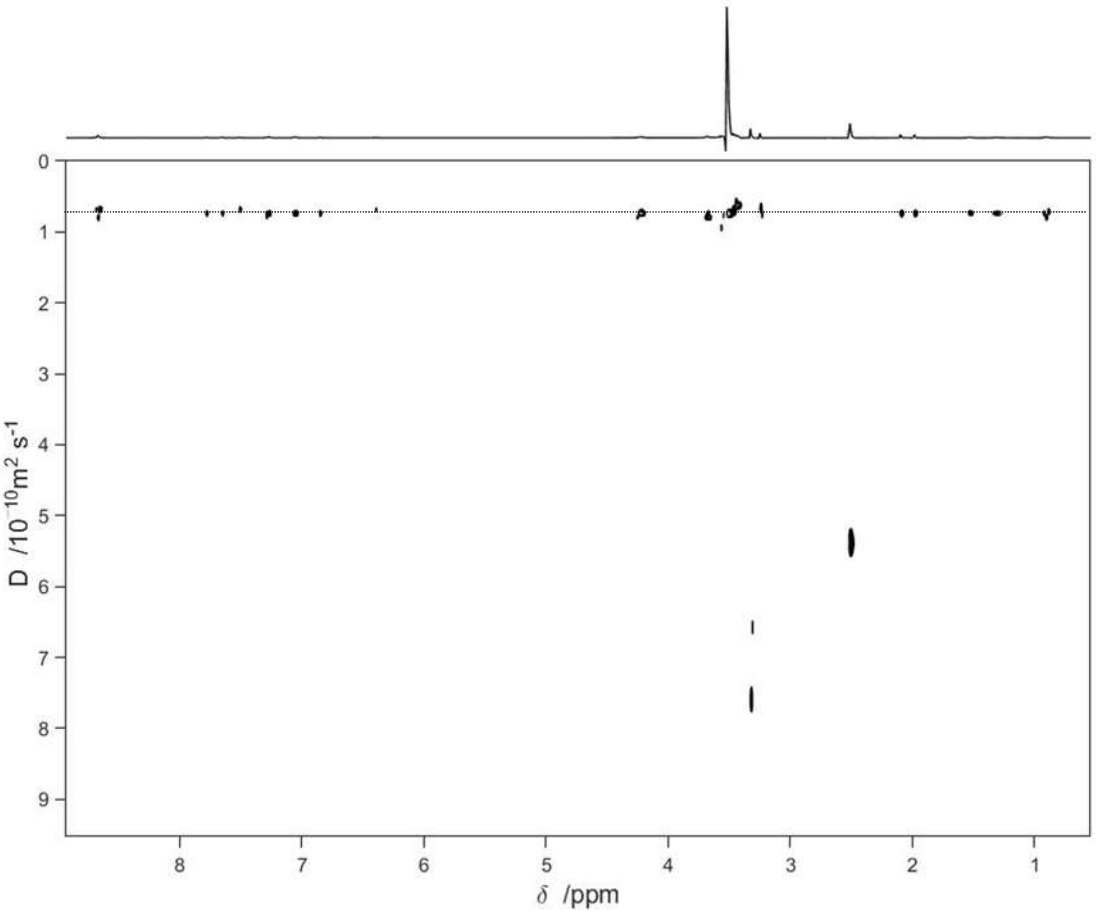

Figure S25. DOSY NMR spectrum of **PEO-NDI-U_2** in DMSO-D_6

2.4.4 Water/DMSO mixtures

PEO-NDI-U_2 was dispersed in water following the DMSO route (dropwise, see SI 2.2). The resulting solution was investigated over time by light scattering and compared to a solution prepared by direct dissolution in water. **Figure S26.*a*** reveals that *ca.* 30 min after preparation, the particles formed by the DMSO route are larger and more aggregated. Nevertheless, solutions prepared by the DMSO route evolved over time contrary to those prepared by direct dissolution in water. After 24 hours, the former reached steady state and the differences with the latter were very weak. We concluded that the DMSO route has no significant impact on the self-assembly of **PEO-NDI-U_2** in aqueous medium at steady state. The initial difference between both preparations methods might be due to formation of aggregates of self-assembled cylinders with the DMSO-route, which eventually become separated into isolated cylinders.

We note that, as for the direct dispersion in water, M_w and R_g obtained for the self-assemblies using the DMSO route was only reproducible within 30%, no matter whether water was added using a syringe-pump or dropwise (data not shown).

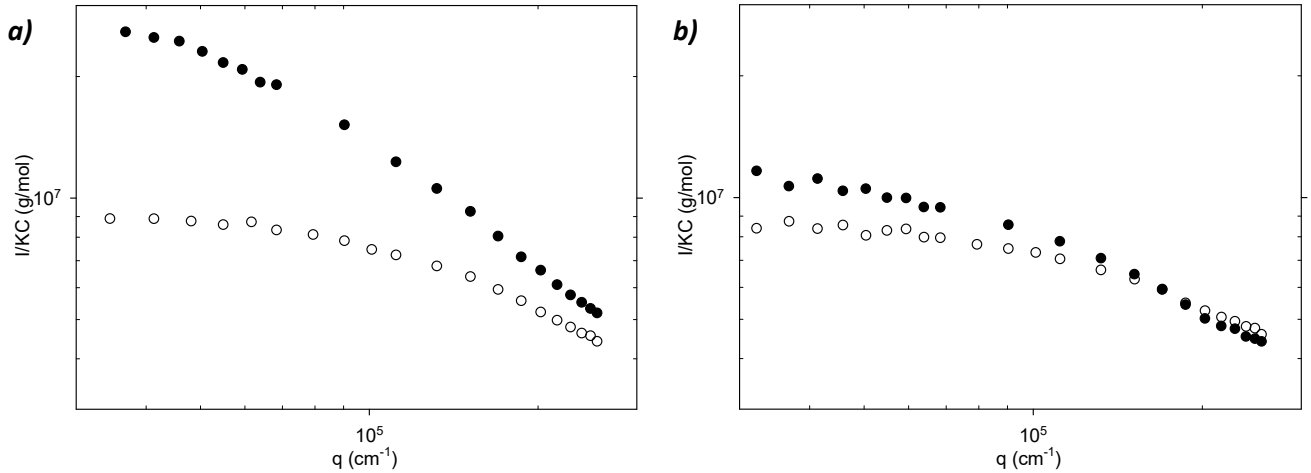

Figure S26. I/KC as a function of q for **PEO-NDI-U_2** solution at 1 g/L (●) in water/DMSO (99/1), (○) in pure water ***a)*** after preparation (30 min) ***b)*** after 24 hours.

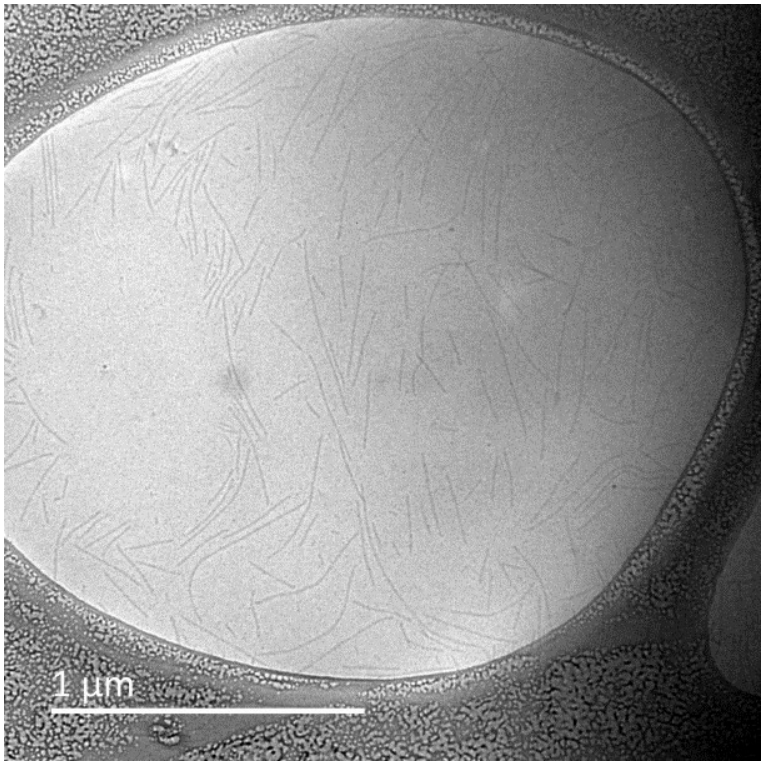

Figure S27. CryoTEM of **PEO-NDI-U_2** in water/DMSO (99/1) (C = 1.3 g/L) after 2 days

2.4.5 Influence of stoppers on the PEO-NDI-U_2 self-assemblies

$H_2PO_4^-$ and urea were previously shown to be very efficient hydrogen bond competitors able to disrupt self-assembled structures based on hydrogen bonding.[23,24] The sensitivity towards these stoppers of the self-assemblies formed by **PEO-NDI-U_2** in aqueous medium was tested in a water-DMSO 99/1 (v/v) mixture. Pre-dispersion in DMSO was selected to start with a solution of unimers and favor interactions between **PEO-NDI-U_2** and the stoppers. For the urea-containing solution, 10 eq. of urea were dissolved in the presence of 1 eq. **PEO-NDI-U_2** in DMSO at a polymer concentration of 100 g/L. After stirring for a few minutes, water was added drop by drop over a few minutes under stirring to reach a water/DMSO ratio of 99/1 by volume and a polymer concentration of 1 g/L. $H_2PO_4^-$ was not soluble in DMSO. Therefore, for the $H_2PO_4^-$-containing solution, 10 eq. of this stopper were first dissolved in 10 µL of water and mixed with 100 µL of a **PEO-NDI-U_2** solution in pure DMSO at 100 g/L. Next, water was added drop by drop to reach a water/DMSO ratio of 99/1 by volume and a polymer concentration of 1 g/L as for the urea-containing solution. Both solutions were analyzed by LS and compared to a solution of **PEO-NDI-U_2** prepared independently in the absence of chain stopper (**Figure S28**). A small difference between the three solutions was observed in SLS, but this difference lies within the variability observed for solutions of **PEO-NDI-U_2** prepared either in pure water or in water/DMSO 99/1 (v/v). Moreover, the particles formed in the presence of 10 eq. of either stopper are clearly still long and strongly aggregated cylinders. As a conclusion, the supramolecular nanocylinders formed by **PEO-NDI-U_2** in aqueous medium are very robust and cannot be destroyed by conventional hydrogen bond competitors. We nevertheless stress that the role of hydrogen bonding in the supramolecular self-assembly of **PEO-NDI-U_2** is crucial since PEO-NDI, lacking the bis(urea) unit, hardly self-assembles in aqueous medium (see SI, section 2.4.7 + **Figure 3**).

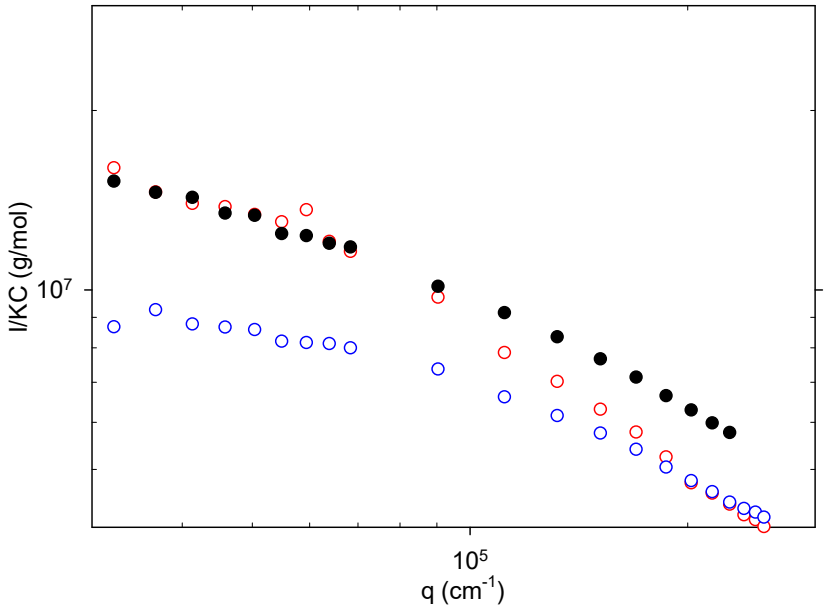

Figure S28. I/KC as a function of q for **PEO-NDI-U_2** solution in water/DMSO (99/1) at 1 g/L (●) without stopper, with 10 equivalents of (○) H_2PO4^-, (○) urea added from the beginning of the preparation of the solution

The lack of sensitivity of **PEO-NDI-U_2** towards hydrogen bond competitors was further confirmed by first forming nanocylinders at 1 g/L of polymer in water and then adding first 10 eq. of $H_2PO_4^-$ and then 10 eq. of urea to the solution of nanocylinders. No change was observed several days after the addition of either stopper (see **Figure S29**).

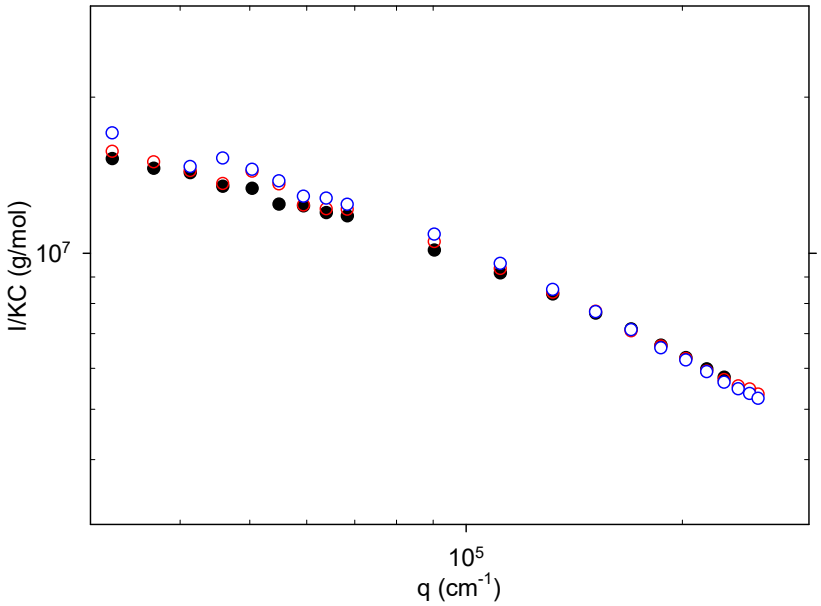

Figure S29. I/KC as a function of q for a **PEO-NDI-U$_2$** solution in water/DMSO (99/1) at 1 g/L (●) without stopper, (○) with 10 eq. of $H_2PO_4^-$, (○) with 10 eq. of $H_2PO_4^-$ + 10 eq. of urea.

2.4.6 Solvent effect

2.4.6.a Water, D_2O, Acetonitrile, Methanol

The self-association of **PEO-NDI-U_2** was also studied by light scattering in deuterated water, methanol and acetonitrile at ~ 2 g/L (see **Figure S30**). The difference between water and deuterated water D_2O was ~ 20%, which was not considered to be significant as it is of the same order of magnitude as the variation observed for independent preparations in water (see part 2.4.1). In methanol and acetonitrile, the extent of self-assembly of **PEO-NDI-U_2** is significant according to the M_w of the scatterers which is much higher than that of POE-NDI-U_2 unimers ($M_{w,unimers}$ ~ 2600 g/mol). However, the aggregation remains much stronger in water and the assembly in methanol or acetonitrile was not studied further.

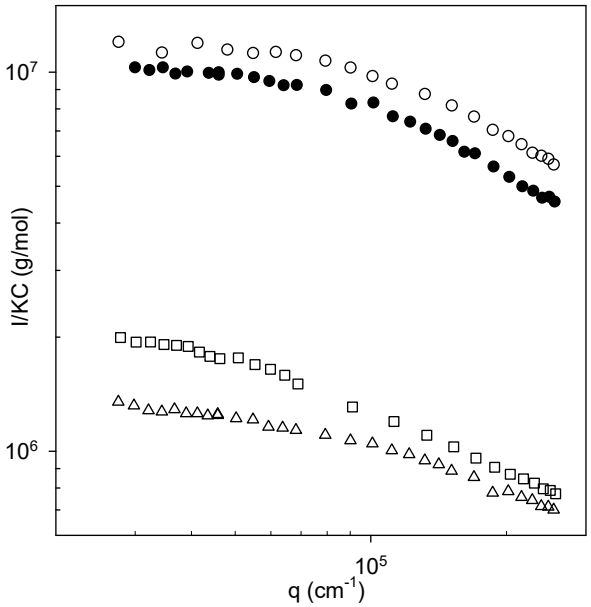

Figure S30. SLS for **PEO-NDI-U_2** at 2.4 g/L in D_2O (○), 1.92 g/L in water (●), 2 g/L in acetonitrile (□), 2.4 g/L in methanol (△)

2.4.6.b Toluene

Study of the self-assembly of **PEO-NDI-U_2** by LS in toluene was not possible considering the very low contrast of the polymer in this solvent (see **Table S2**). However, it could be investigated in toluene-d_8 at 10 g/L and 5 g/L by SANS (see **Figure S31**). A small difference of I/KC was observed between 10 and 5 g/L hinting at a weak concentration effect probably due to repulsive interactions between the assemblies at high concentration. The scattered intensity was close to a q^{-1}-dependency, particularly at C = 5 g/L where repulsive interactions are less important, which is consistent with the formation of cylinders in toluene too.

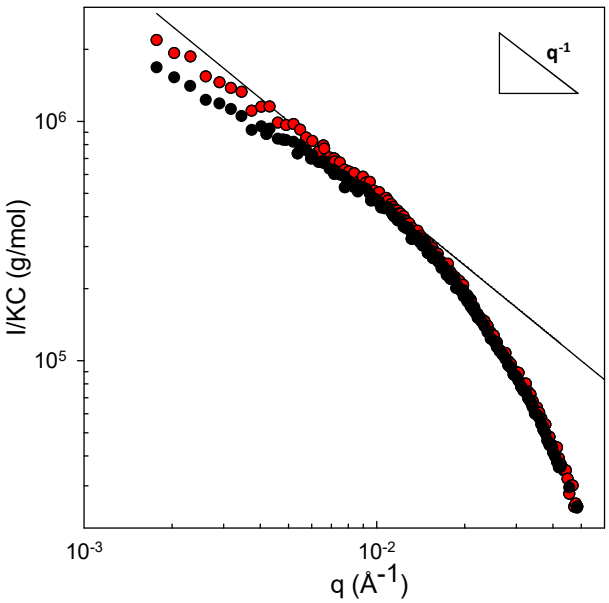

Figure S31. I/KC as a function of q for **PEO-NDI-U$_2$** in toluene-d$_8$ at 10 g/L (●) and 5 g/L (●)

2.4.7 CryoTEM of PEO-NDI

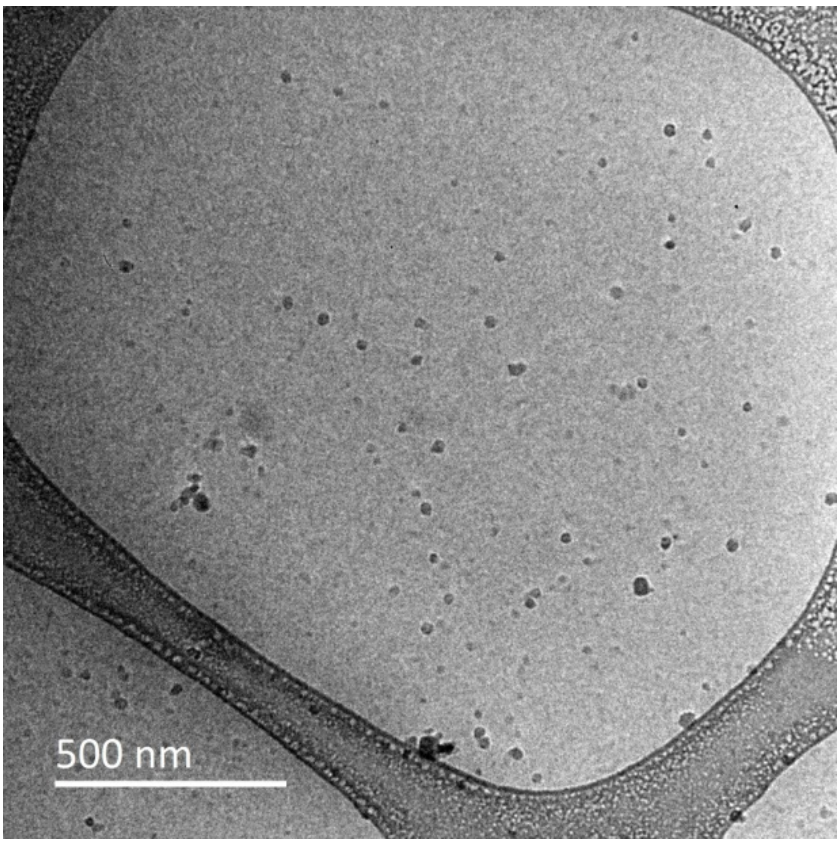

Figure S32. CryoTEM of **PEO-NDI** in water (C = 1 g/L)

2.5 Dimensions of PEO-NDI-U2

The R_h of **PEO-NDI-U2** unimer in DMSO was estimated to be 2.5 nm. In these conditions, the PEO arm assumes a Gaussian conformation which sets the lower limit of the size of a single **PEO-NDI-U2** molecule at 2 × R_h(unimer) = 5 nm. The upper limit of the size of a **PEO-NDI-U2** molecule was estimated by modelisation in Spartan with a fully stretched PEO arm at 19 nm. The radius of the speculative model proposed in **Figure 4** should therefore lie between 5 and 19 nm which is in agreement with the value found by SANS.

References

1 P. Mongondry, C. Bonnans-Plaisance, M. Jean and J. F. Tassin, *Macromol. Rapid Commun.*, 2003, **24**, 681–685.
2 B. A. Ikkanda, S. A. Samuel and B. L. Iverson, *J. Org. Chem.*, 2014, **79**, 2029–2037.
3 R. Siegrist, D. Pozzi, G. Jacob, C. Torrisi, K. Colas, B. Braibant, J. Mawet, T. Pfeifer, R. de Kanter, C. Roch, M. Kessler, O. Corminboeuf and O. Bezençon, *J. Med. Chem.*, 2016, **59**, 10661–10675.
4 M. Kudo, K. Katagiri, I. Azumaya, H. Kagechika and A. Tanatani, *Tetrahedron*, 2012, **68**, 4455–4463.
5 C. Fonteneau, S. Pensec and L. Bouteiller, *Polym. Chem.*, 2014, **5**, 2496–2505.
6 W. Brown, Ed., *Dynamic Light Scattering: The Method and Some Applications*, Oxford University Press, Oxford, New York, 1993.
7 C. Y. Young, P. J. Missel, N. A. Mazer, G. B. Benedek and M. C. Carey, *J. Phys. Chem.*, 1978, **82**, 1375–1378.
8 K. Schillen, W. Brown and R. M. Johnsen, *Macromolecules*, 1994, **27**, 4825–4832.
9 C. Charbonneau, M. M. D. S. Lima, C. Chassenieux, O. Colombani and T. Nicolai, *Phys. Chem. Chem. Phys.*, 2013, **15**, 3955–3964.
10 C. Lefay, B. Charleux, M. Save, C. Chassenieux, O. Guerret and S. Magnet, *Polymer*, 2006, **47**, 1935–1945.
11 E. Lejeune, C. Chassenieux and O. Colombani, in *Trends in Colloid and Interface Science XXIV*, eds. V. Starov and K. Procházka, Springer Berlin Heidelberg, 2011, pp. 7–16.
12 C. Chassenieux, T. Nicolai and D. Durand, *Macromolecules*, 1997, **30**, 4952–4958.
13 S. Han, E. Nicol, F. Niepceron, O. Colombani, S. Pensec and L. Bouteiller, *Macromol. Rapid Commun.*, 2019, **40**, 1800698.
14 J. Brandrup, E. H. Immergut and E. A. Grulke, *Polymer Handbook, 4th Edition*, Wiley, 1998.
15 W. Brown, *Light Scattering: Principles and Development*, Clarendon Press, Oxford,U.K., 1996, vol. 53.
16 J. S. Pedersen, *Adv. Colloid Interface Sci.*, 1997, **70**, 171–210.
17 P. Terech and A. Coutin, *Langmuir*, 1999, **15**, 5513–5525.
18 F. Lortie, S. Boileau, L. Bouteiller, C. Chassenieux, B. Demé, G. Ducouret, M. Jalabert, F. Lauprêtre and P. Terech, *Langmuir*, 2002, **18**, 7218–7222.
19 J. Pérez-Folch, J. A. Subirana and J. Aymami, *J. Chem. Crystallogr.*, 1997, **27**, 367–369.
20 T. Nicolai, O. Colombani and C. Chassenieux, *Soft Matter*, 2010, **6**, 3111–3118.
21 W. Schnabel and Borgward.u, *Macromol. Chem. Phys.*, 1969, **123**, 73–79.
22 P. Choudhury, K. Das and P. K. Das, *Langmuir*, 2017, **33**, 4500–4510.
23 T. Pinault, C. Cannizzo, B. Andrioletti, G. Ducouret, F. Lequeux and L. Bouteiller, *Langmuir*, 2009, **25**, 8404–8407.
24 P. Rajdev, M. R. Molla and S. Ghosh, *Langmuir*, 2014, **30**, 1969–1976.